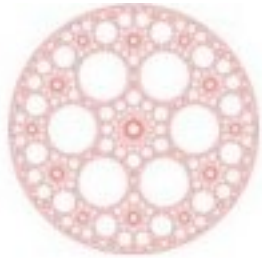


From thermal rectifiers to thermoelectric devices



Giuliano Benenti

Center for Nonlinear and Complex Systems,
Univ. Insubria, Como, Italy
INFN, Milano, Italy

OUTLINE

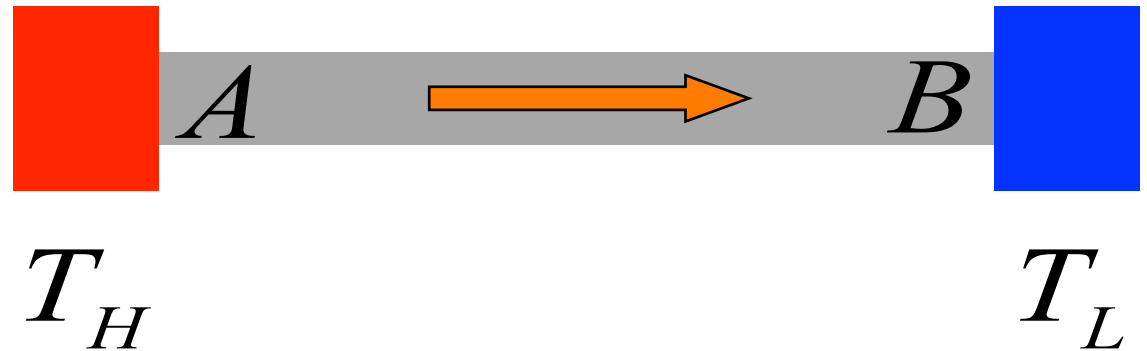
Can we derive the **Fourier law** of heat conduction from **dynamical** equations of motion, without any a priori statistical assumptions? And in quantum mechanics?

Can we control the heat current? Towards **thermal diodes** and **thermal transistors**

Coupled heat and charge transport: mechanisms for optimizing the figure of merit of **thermoelectric efficiency**

Fourier Heat Conduction Law (1808)

“Théorie de la Propagation de la Chaleur dans les Solides”



$$J = -\kappa \nabla T$$

J : heat flux

∇T : temperature gradient

κ : thermal conductivity

An old problem, and a long history

1808 - J.J. Fourier: study of the earth thermal gradient

19 century: Clausius, Maxwell, Boltzmann,
kinetic theory of gas, Boltzmann transport equation

1914 - P. Debye: $\kappa \sim Cvl$, conjectured the role of nonlinearity to ensure finite transport coefficients

1936 - R. Peierls: reconsidered Debye's conjecture

1953 - E. Fermi, J. Pasta and S.Ulam: **(FPU) numerical experiment** to verify Debye's conjecture

“It seems there is no problem in modern physics for which there are on record as many false starts, and as many theories which overlook some essential feature, as in the problem of the thermal conductivity of (electrically) nonconducting crystals.”

R. E. Peierls (1961),
Theoretical Physics in the Twentieth Century.

QUESTION:

Can one derive the Fourier law of heat conduction from **dynamical** equations of motion without any statistical assumption?

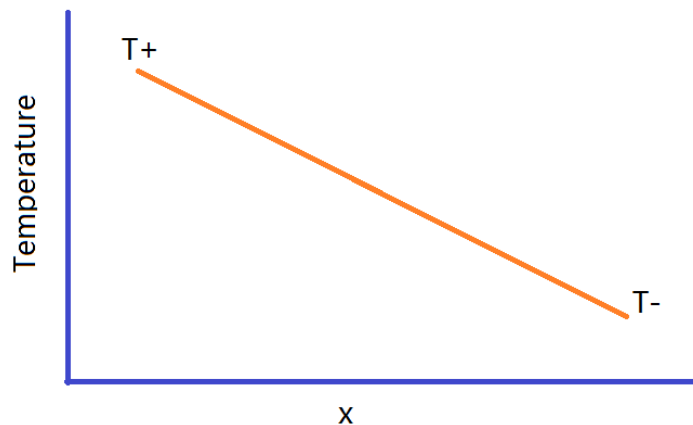
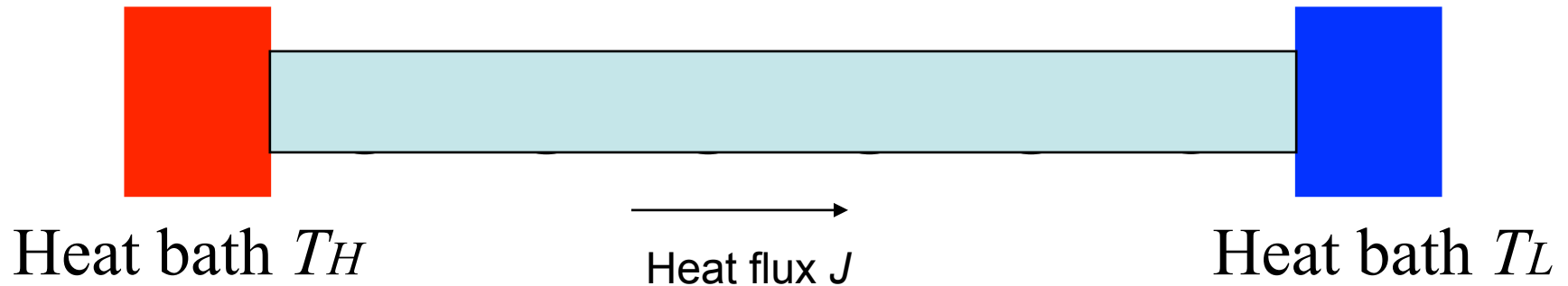
REMARK:

(Normal) heat flow obeys a simple diffusion equation which can be regarded as a continuous limit of a discrete random walk

Randomness should be an essential ingredient of thermal conductivity

deterministically random systems are tacitly required by the transport theory

Methods: nonequilibrium simulations



$$J = -\kappa \nabla T \rightarrow \kappa \approx -\frac{JL}{\Delta T}$$

S. Lepri, et al, Phys. Rep. 377, 1 (2003); A. Dhar, Adv. Phys. 57, 457 (2008)



Ding-a-ling model



chaos for $\omega^2/E \gg 1$

Free electron gases at the reservoirs with Maxwellian distribution of velocities

$$f(v) = \frac{m |v|}{T} \exp\left(-\frac{mv^2}{2T}\right)$$

Heat flux $J = \lim_{t \rightarrow \infty} \frac{1}{t} \sum_i \Delta E_i$

Internal temperature $T_i = \langle v_i^2 \rangle$ ($m = k_B = 1$)

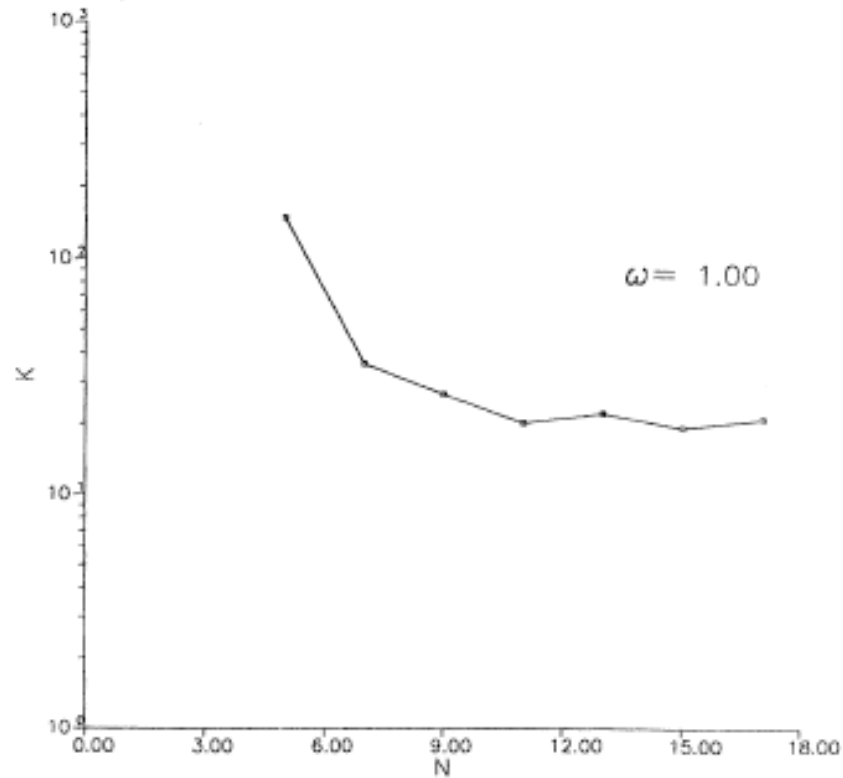


FIG. 3. Behavior of the coefficient of thermal conductivity as a function of the particle number N .

(G. Casati, J. Ford, F. Vivaldi, W.M. Visscher, PRL **52**, 1861 (1984))

Methods: equilibrium simulations

Green-Kubo formula:

$$\kappa_{GK} = \lim_{\tau \rightarrow \infty} \lim_{N \rightarrow \infty} \frac{1}{T^2 N} \int_0^\tau \langle J(t)J(0) \rangle dt ,$$

$$J(t) = \sum_{i=1}^N J_i(t)$$

$$\langle J(t)J(0) \rangle / N \sim t^{-\gamma} \quad \left\{ \begin{array}{l} 0 \leq \gamma \leq 1 \quad \text{anomalous heat conduction} \\ \gamma > 1 \quad \text{normal heat conduction} \end{array} \right.$$

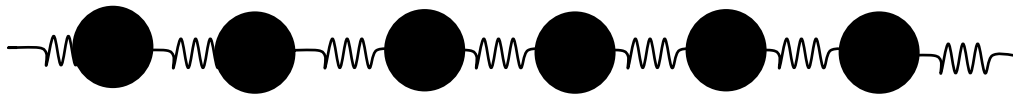
S. Lepri, et al, Phys. Rep. 377, 1 (2003); A. Dhar, Adv. Phys. 57, 457 (2008)

Momentum-conserving systems

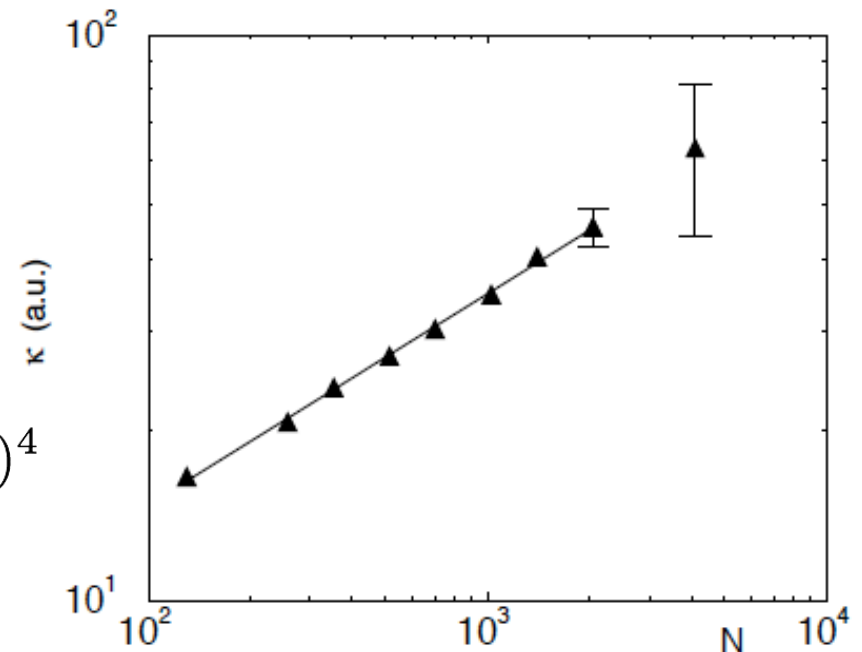
Slow decay of correlation functions, diverging transport coefficients

(Alder and Wainwright, PRA **1**, 18 (1970))

FPU revisited: chaos is not sufficient to obtain Fourier law
(Lepri, Livi, Politi, EPL **43**, 271 (1998))



$$V(y_n - y_{n-1}) = \frac{1}{2} K (y_n - y_{n-1})^2 + \frac{1}{4} g (y_n - y_{n-1})^4$$



For momentum-conserving systems

3D $\kappa \sim L^0$ (normal heat conduction)

{ 2D $\kappa \sim \ln(L)$ (anomalous heat conduction)

{ 1D $\kappa \sim L^\alpha$ (anomalous heat conduction)

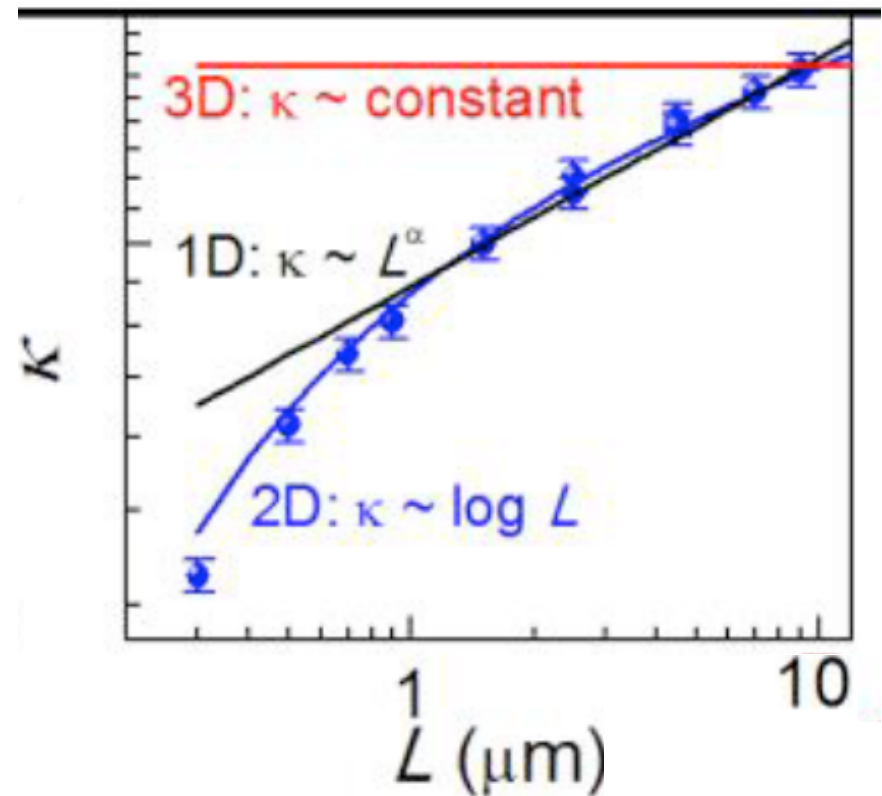
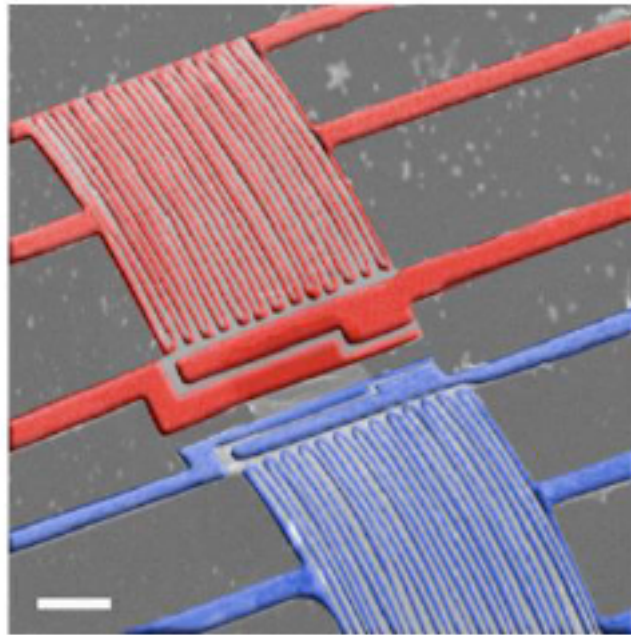
From hydrodynamic theory: $\alpha = 1/3$

Length-dependent thermal conductivity in suspended single-layer graphene

Xiangfan Xu, Luiz F. C. Pereira, Yu Wang, Jing Wu, Kaiwen Zhang, Xiangming Zhao, Sukang Bae, Cong Tinh Bui, Rongguo Xie, John T. L. Thong, Byung Hee Hong, Kian Ping Loh, Davide Donadio, Baowen Li & Barbaros Özyilmaz

Nature Communications 5, Article number: 3689 doi:10.1038/ncomms4689

Received 09 October 2013 Accepted 19 March 2014 Published 16 April 2014



The red and blue Pt coils are the heater and sensor thermally connected by suspended graphene (grey sheet in the middle)

Fourier law in quantum mechanics

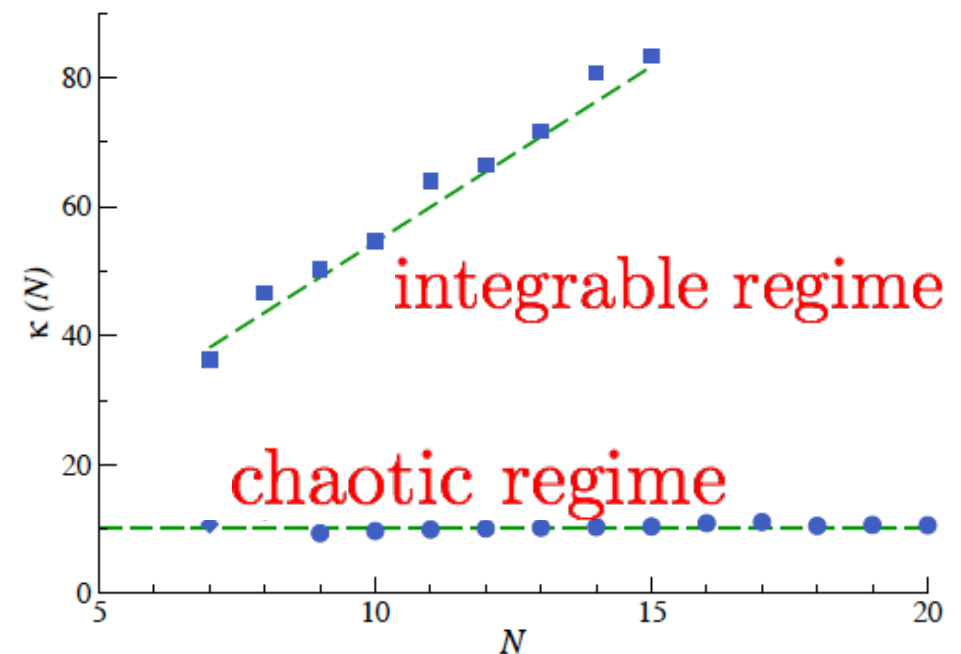
Quantum chaos ensures diffusive heat transport and decay of “dynamical” (energy-energy) correlation functions.

Exponential sensitivity to errors absent in quantum mechanics but not necessary to obtain the Fourier law



$$\mathcal{H} = \sum_{n=0}^{N-2} H_n + \frac{\hbar}{2} (\sigma_L + \sigma_R),$$

$$H_n = -Q\sigma_n^z \sigma_{n+1}^z + \frac{\hbar}{2} \cdot (\sigma_n + \sigma_{n+1})$$



Can we control the heat current?

Towards thermal diodes and thermal transistors

Thermal rectification: everyday's experience when there is **thermal convection** (transfer of matter, e.g.: heating a **fluid** from below or from the top surface)

Thermal rectifiers much less intuitive in **solid-state devices**, but not forbidden by thermodynamics

Let us focus on **electrical insulators** (heat carried by lattice vibrations: **phonons**)

Rectification factor

Ratio between reverse and forward heat flow

$$R = \left| \frac{j_r}{j_f} \right| \quad (\text{assuming } j_r > j_f)$$

Why can these flows be different?

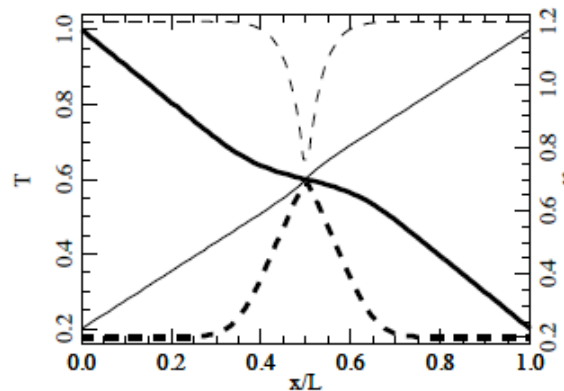
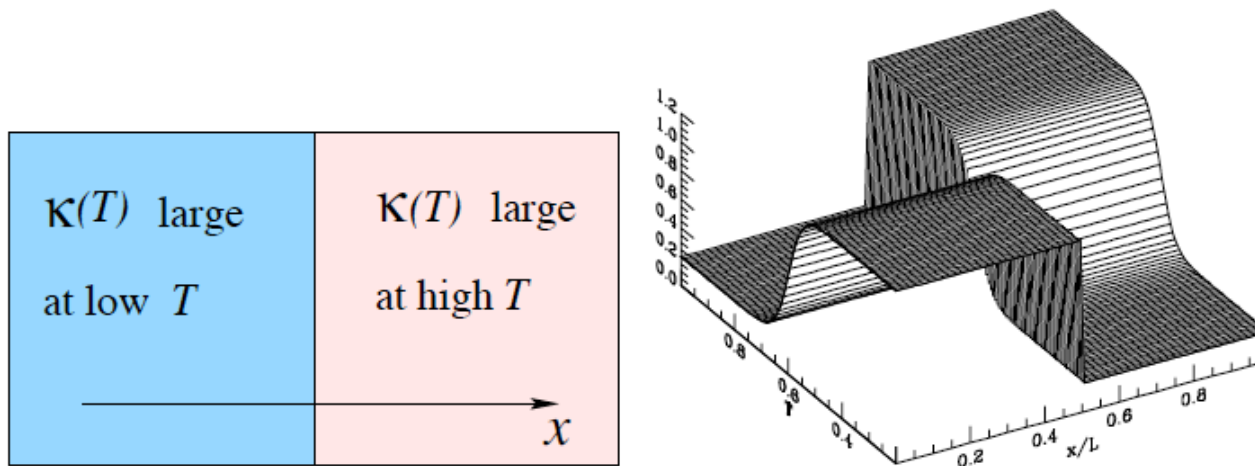
Assuming the Fourier law:

$$T(x) = T_1 + \int_0^x \frac{j_f}{\kappa[\xi, T(\xi)]} d\xi \quad T(x=L) = T_2$$

reversing boundary conditions we can change temperature and local thermal conductivity distributions

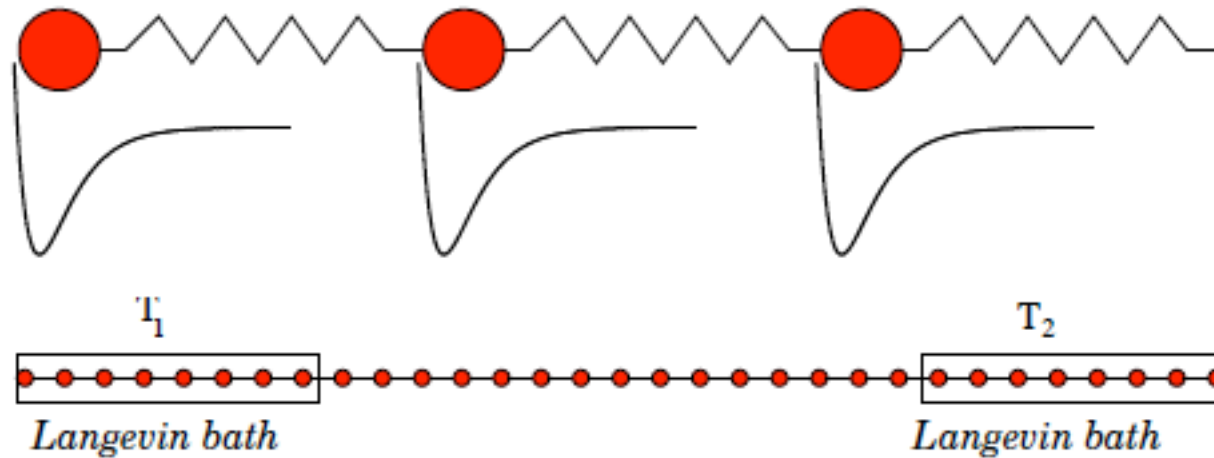
Two ingredients are needed:

- Temperature-dependent thermal conductivity
- breaking of the inversion symmetry of the device in the direction of the flow



$$R = |j_r/j_f| = 4.75$$

Microscopic model



$$\mathcal{H} = \sum_{n=1}^N H_n = \sum_{n=1}^N \left[\frac{p_n^2}{2m} + \frac{1}{2}K(y_n - y_{n-1})^2 + D_n(e^{-\alpha_n y_n} - 1)^2 \right]$$

Morse on-site potential: **Nonlinearity** needed to have temperature-dependent phonon bands

Linearized model (around the equilibrium position):

$$H = \sum_n \frac{p_n^2}{2m} + \tilde{D}_n y_n^2 + \frac{1}{2} K (y_n - y_{n-1})^2$$
$$\tilde{D}_n = D_n \alpha_n^2$$

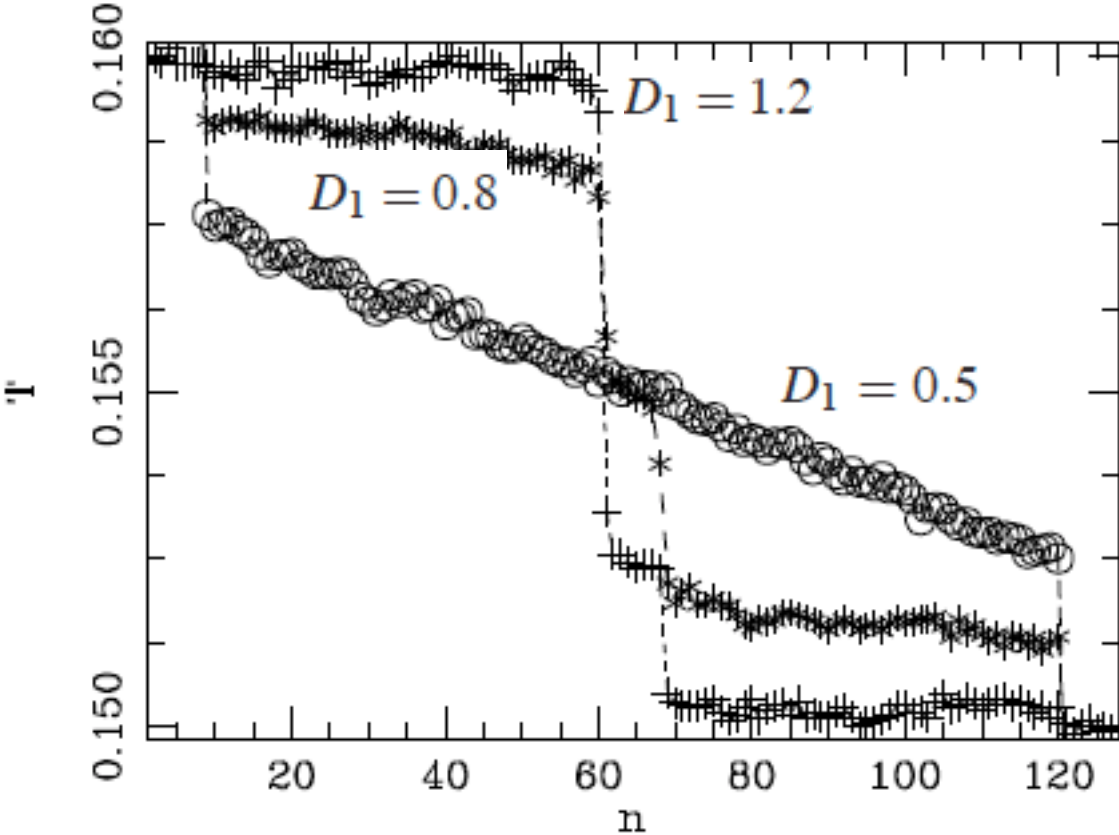
$$y_n(t) = e^{ikn - i\omega t} \quad \text{Plane waves solutions}$$

$$\omega^2 = 2K + 2\tilde{D} - 2K \cos k \quad \text{Dispersion relations}$$

$$2\tilde{D} \leq \omega^2 \leq 2\tilde{D} + 4K \quad \text{Phonon band}$$

phonon-band mismatch:

$D = 0.5$	$\alpha = 1.0$	D_1	$D = 0.5$	$\alpha = 1.0$
$K = 0.30$		$\alpha = 1.0$	$K = 0.30$	
		$K = 0.30$		

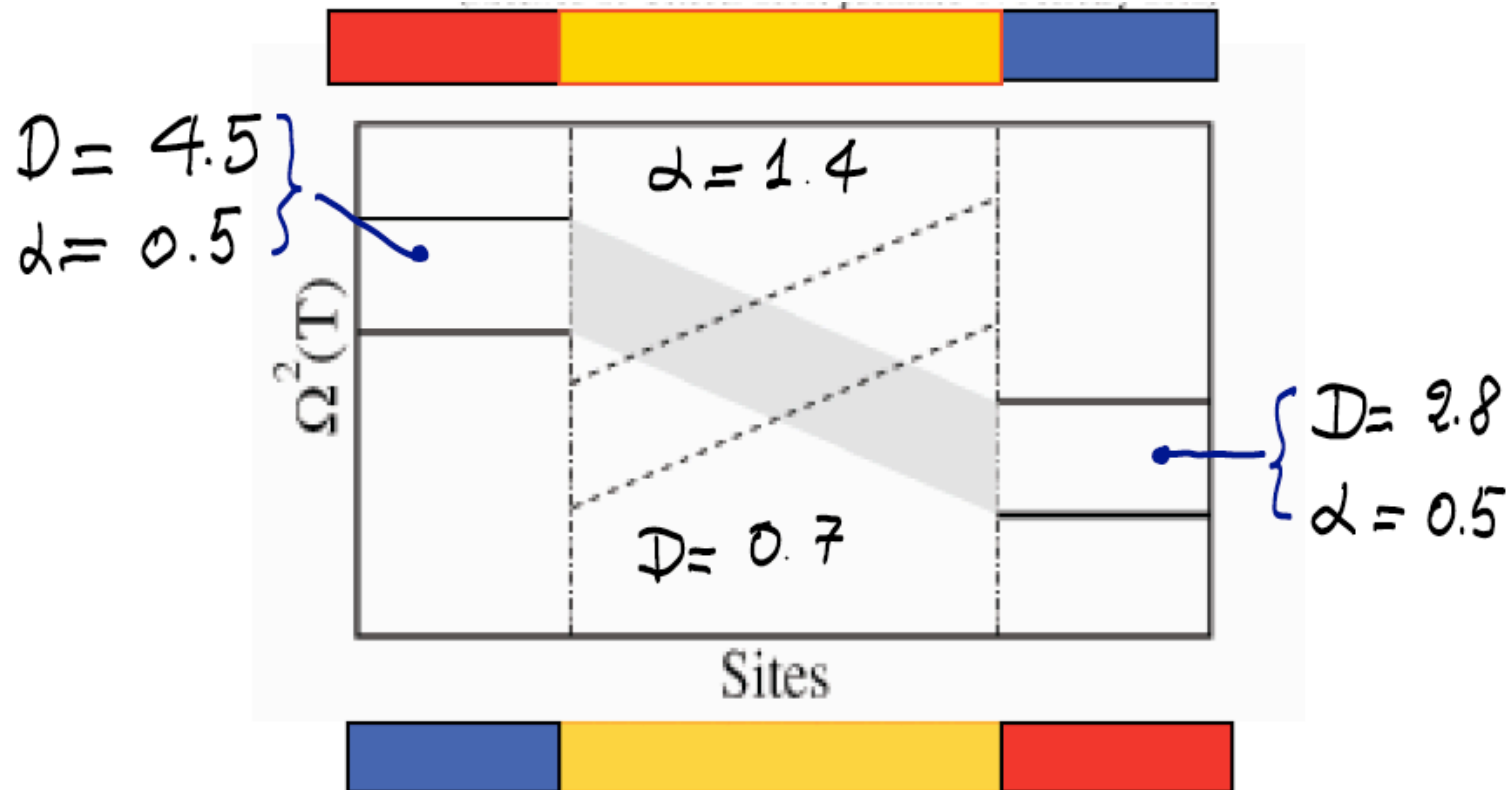


Effective (temperature-dependent) harmonic model:

$$H_0 = \sum_{n=1,N} \frac{p_n^2}{2m} + \Omega^2(T)y_n^2 + \frac{1}{2} \Phi(T) (y_n - y_{n-1})^2$$

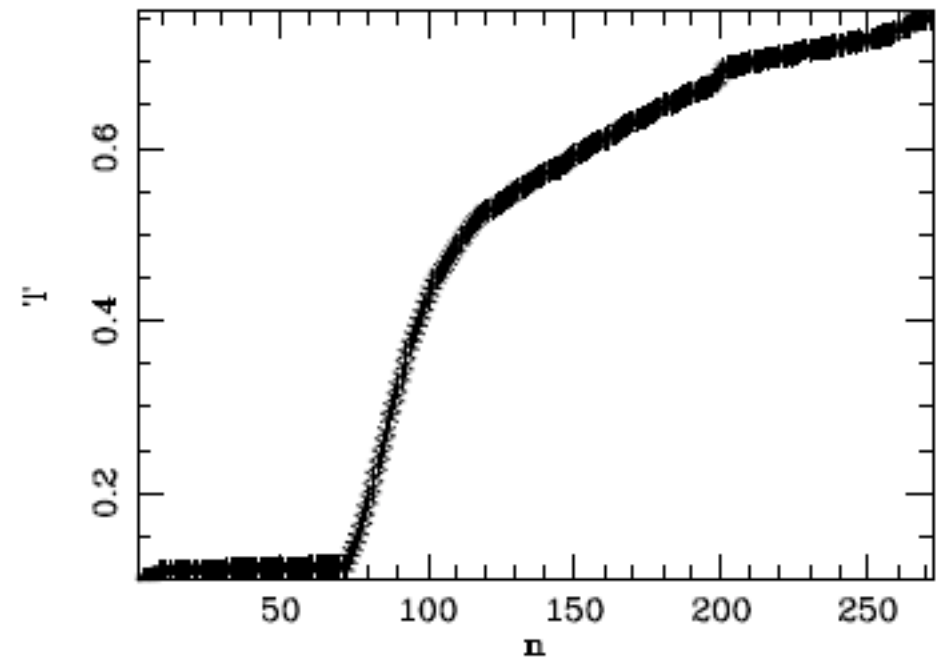
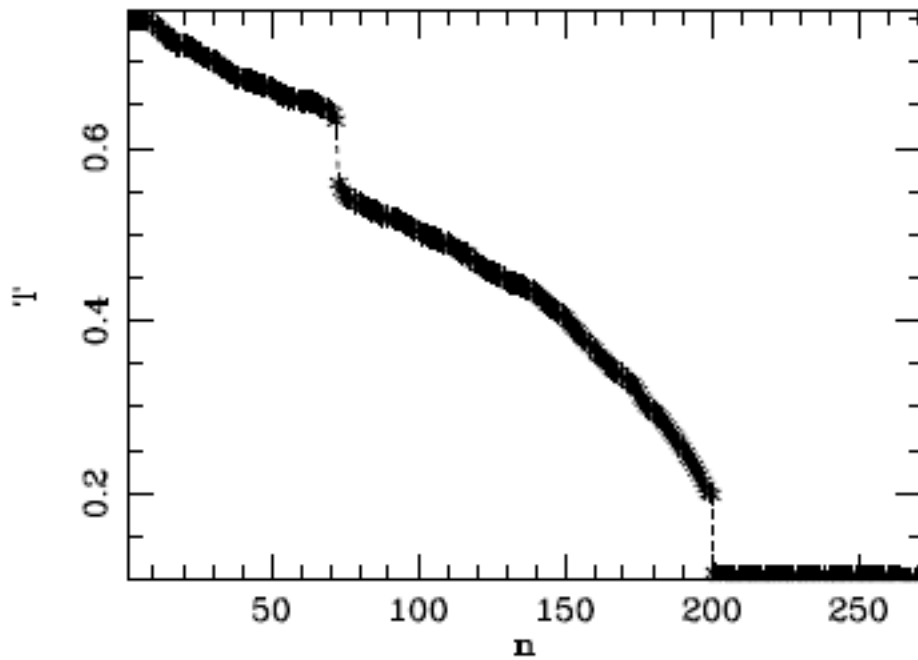
$$\Phi(T) = K$$

$\Omega(T)$ decreases as T increases



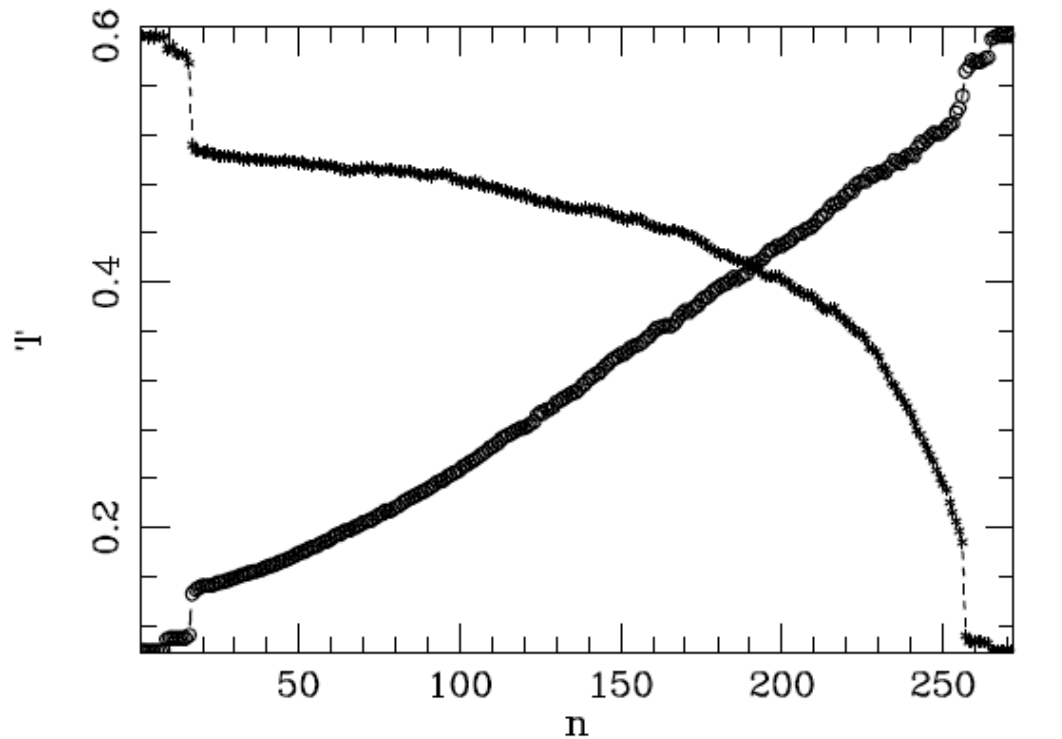
(M. Terraneo, M. Peyrard, G. Casati, PRL **88**, 094302 (2002))

large interface (Kapitza) resistance



$$|j_{\text{right} \rightarrow \text{left}}| / j_{\text{left} \rightarrow \text{right}} = 2.4$$

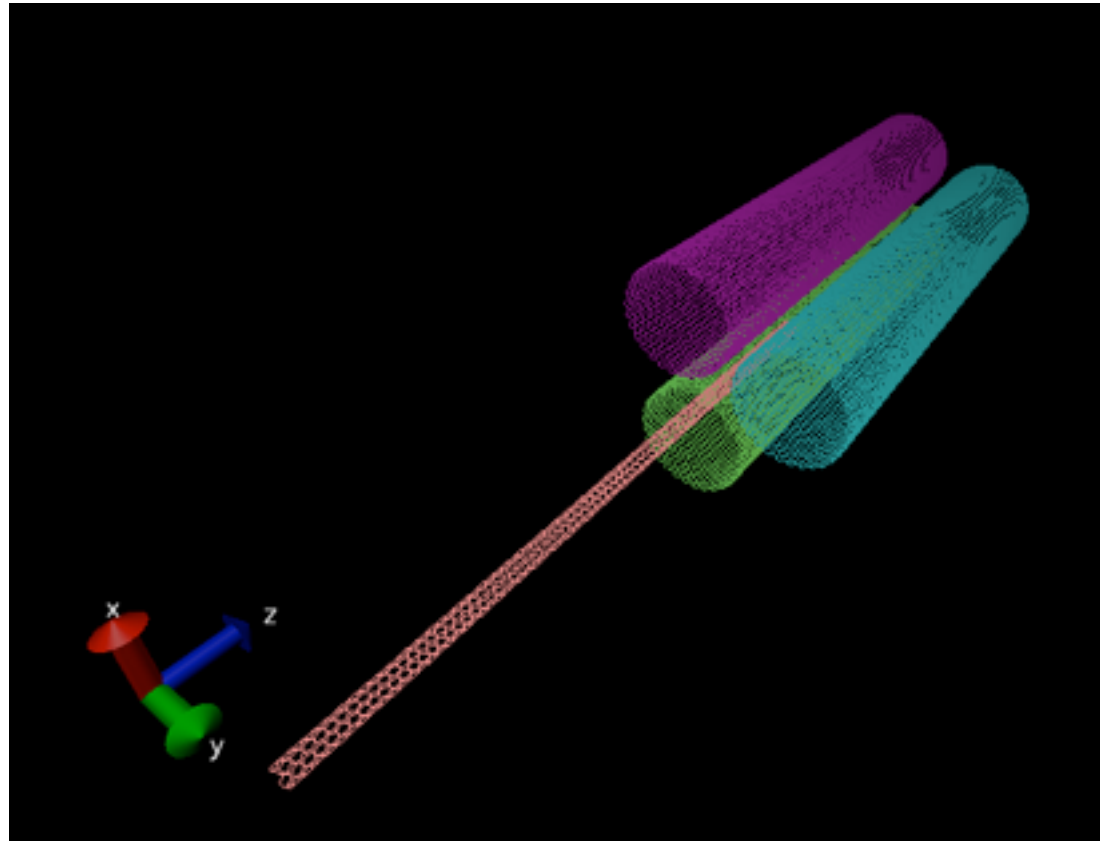
With continuous variation of the vibrational properties versus space (it amounts to stacking an infinity of interfaces):



rectifying coefficient $R = 4.95$

(for a pedagogical review, see G. B., G. Casati, C. Mejia-Monasterio, M. Peyrard, in Lecture Notes in Physics, in press)

A different model: carbon nanotube bundles



Interplay between Kapitza resistance and thermal rectification. R up to 1.2 (work in progress)

Solid-State Thermal Rectifier

C. W. Chang,^{1,4} D. Okawa,¹ A. Majumdar,^{2,3,4} A. Zettl^{1,3,4*}

SCIENCE VOL 314 17 NOVEMBER 2006

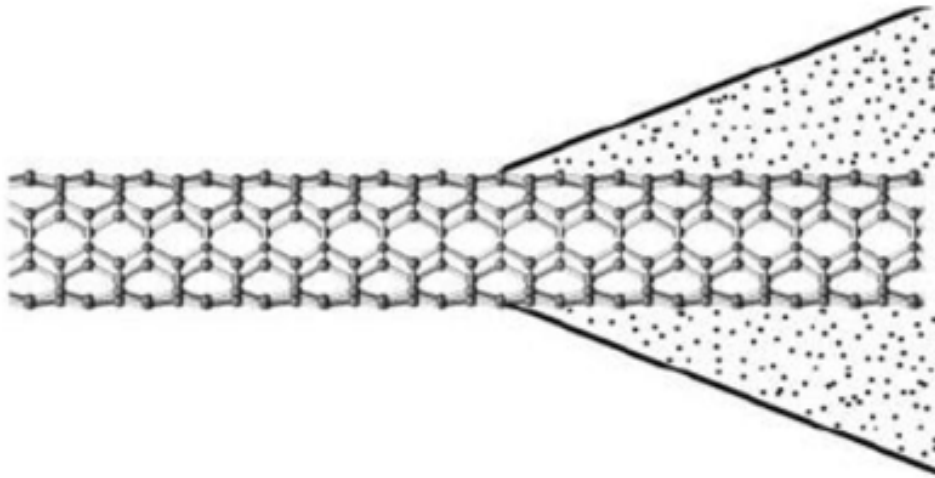


Fig. 1. A schematic description of depositing amorphous C₉H₁₆Pt (black dots) on a nanotube (lattice structure).

For **uniform mass distribution**, thermal conduction is symmetric.

For **mass loading geometry** higher thermal conductance was observed when heat flowed from the high-mass region to the low-mass region.

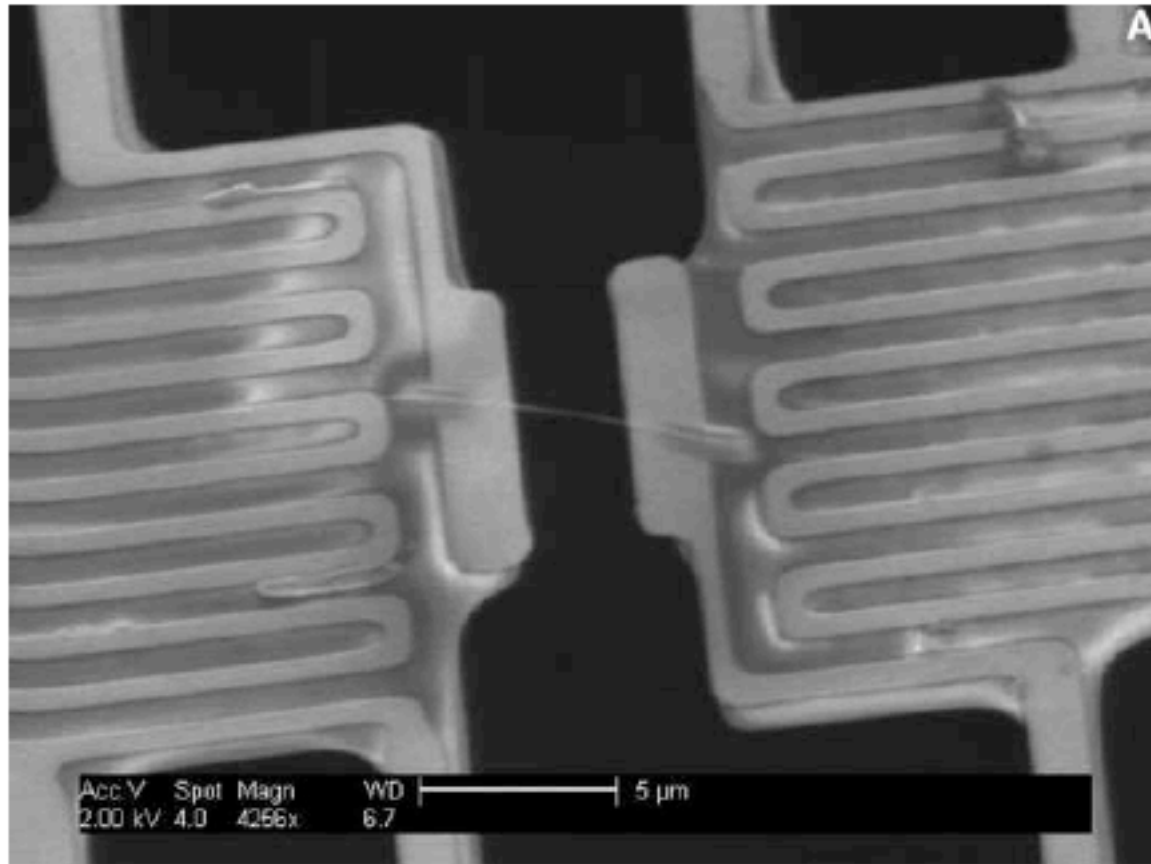
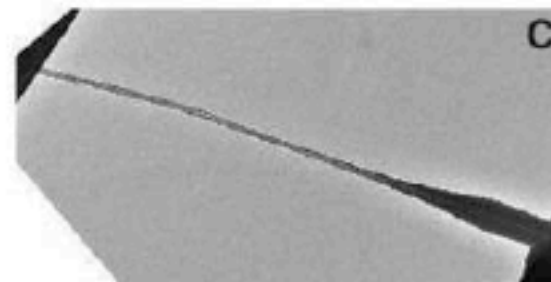
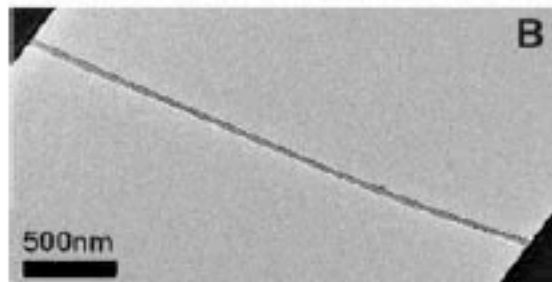


Fig. 2. (A) The SEM image of a CNT (light gray line in center) connected to the electrodes. Scale bar, 5 μm. (B and C) The corresponding low-magnification TEM images of the same CNT in (A), before (B) and after (C) C₉H₁₆Pt was deposited.



thermal rectifications

7, 4, and 3%

An oxide thermal rectifier

W. Kobayashi,^{1,a)} Y. Teraoka,² and I. Terasaki³

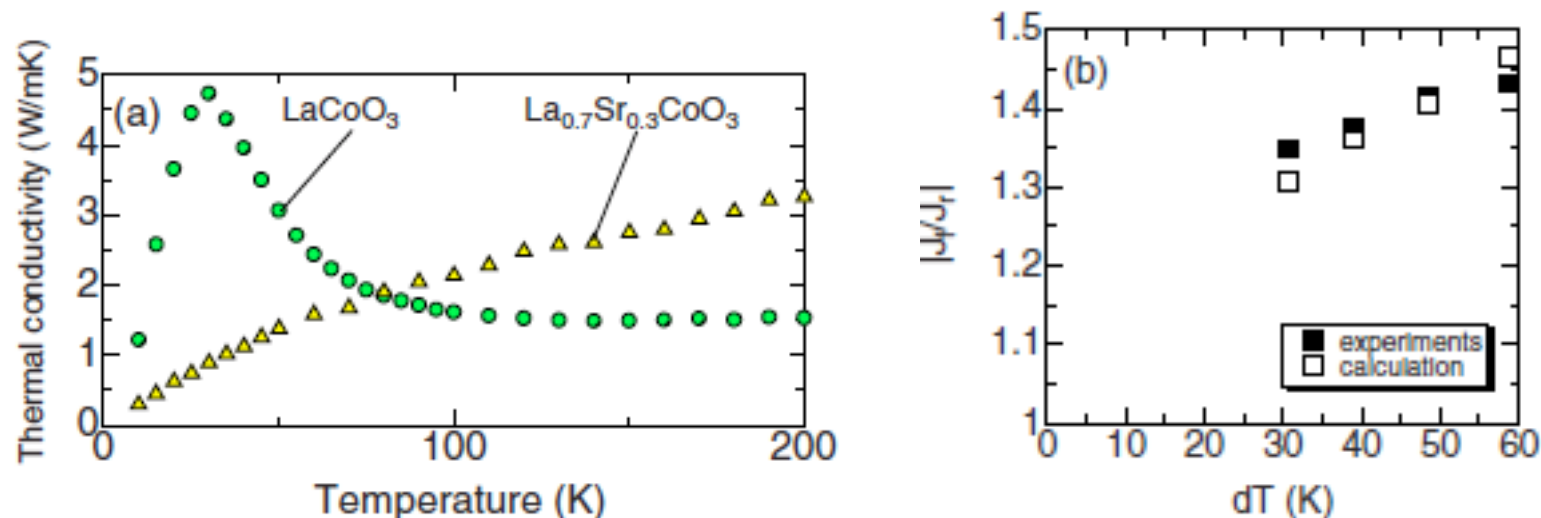
¹Waseda Institute for Advanced Study, Waseda University, Tokyo 169-8050, Japan and PRESTO, Japan Science and Technology Agency, Saitama 332-0012, Japan

²Department of Physics, Waseda University, Tokyo 169-8555, Japan

³Department of Applied Physics, Waseda University, Tokyo 169-8555, Japan

(Received 13 June 2009; accepted 2 October 2009; published online 29 October 2009)

We have experimentally demonstrated thermal rectification as bulk effect. According to a theoretical design of a thermal rectifier, we have prepared an oxide thermal rectifier made of two cobalt oxides with different thermal conductivities, and have made an experimental system to detect the thermal rectification. The rectifying coefficient of the device is found to be 1.43, which is in good agreement with the numerical calculation. © 2009 American Institute of Physics. [doi:10.1063/1.3253712]



Thermal Rectification in the Vicinity of a Structural Phase Transition

Wataru Kobayashi^{1,2,3*}, Daisuke Sawaki⁴, Tsubasa Omura⁴, Takuro Katsufuji⁴,
Yutaka Moritomo^{1,2}, and Ichiro Terasaki⁵

¹Graduate School of Pure and Applied Sciences, University of Tsukuba, Ibaraki 305-8571, Japan

²Tsukuba Research Center for Interdisciplinary Materials Science (TIMS), University of Tsukuba, Ibaraki 305-8571, Japan

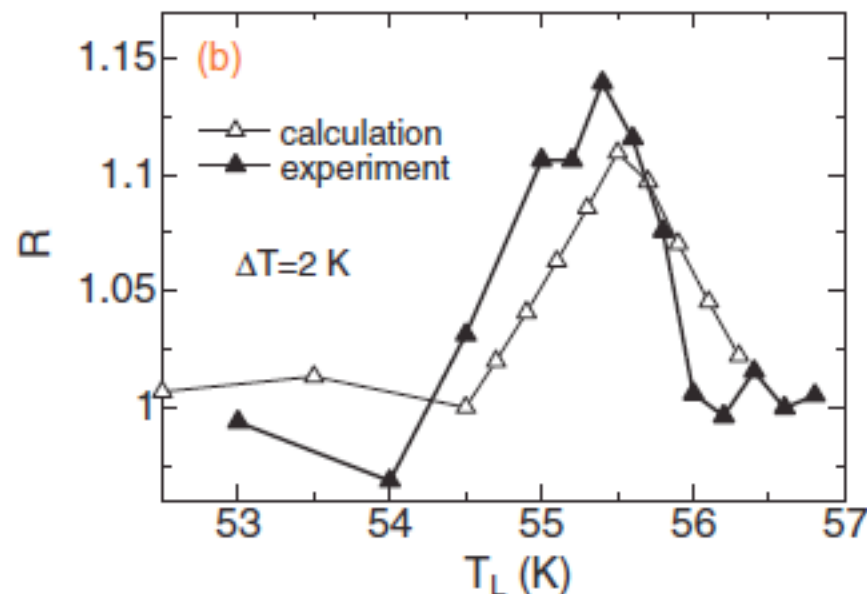
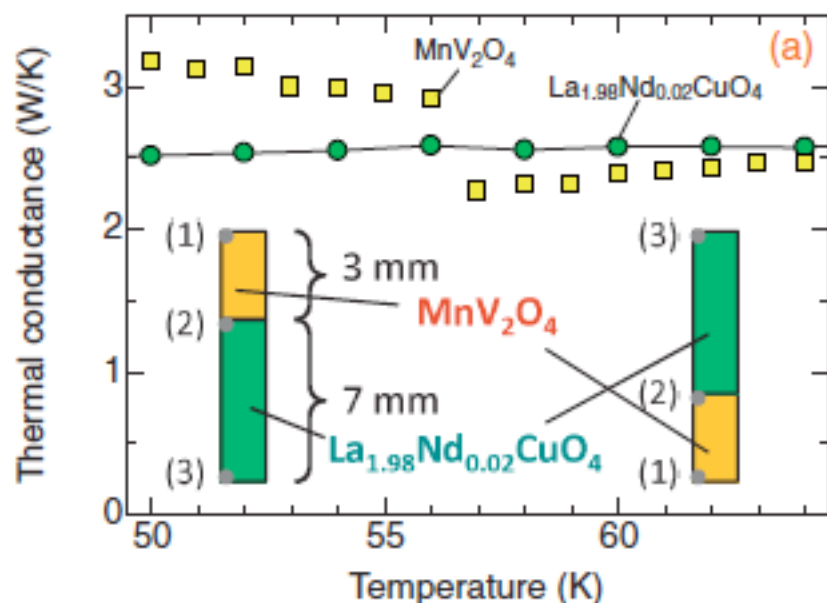
³PRESTO, Japan Science and Technology Agency, Kawaguchi, Saitama 332-0012, Japan

⁴Department of Physics, Waseda University, Shinjuku, Tokyo 169-8555, Japan

⁵Department of Physics, Nagoya University, Nagoya 464-8602, Japan

Received December 7, 2011; accepted January 5, 2012; published online January 25, 2012

We have fabricated an oxide thermal rectifier made of $\text{La}_{1.98}\text{Nd}_{0.02}\text{CuO}_4$ and MnV_2O_4 . By utilizing a jump of a thermal conductivity originated in the structural phase transition accompanied by the orbital ordering in MnV_2O_4 , a rectifying coefficient of 1.14 has been achieved in the presence of a small temperature difference of 2 K. A thermal rectifier operating under a small temperature difference will play an important role for realizing heat-current control in electronic devices. © 2012 The Japan Society of Applied Physics

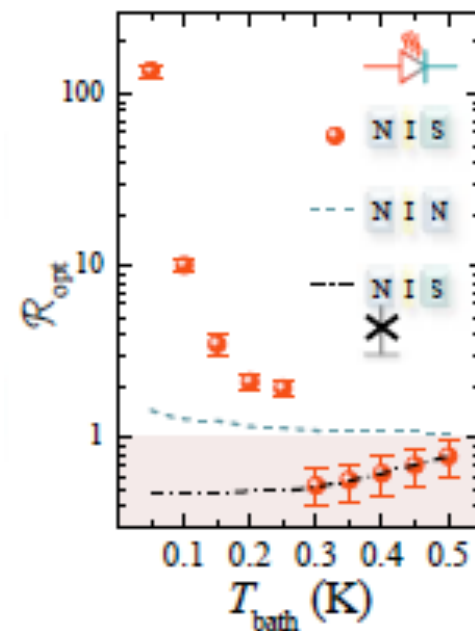
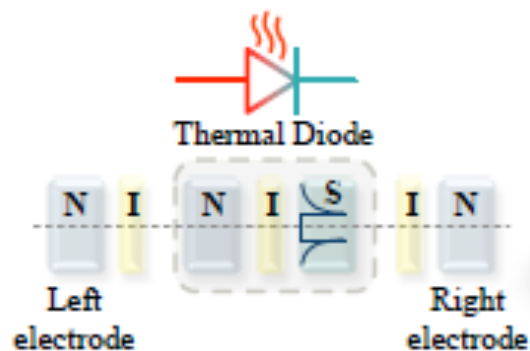


Rectification of electronic heat current by a hybrid thermal diode

Maria José Martínez-Pérez, Antonio Fornieri & Francesco Giazotto

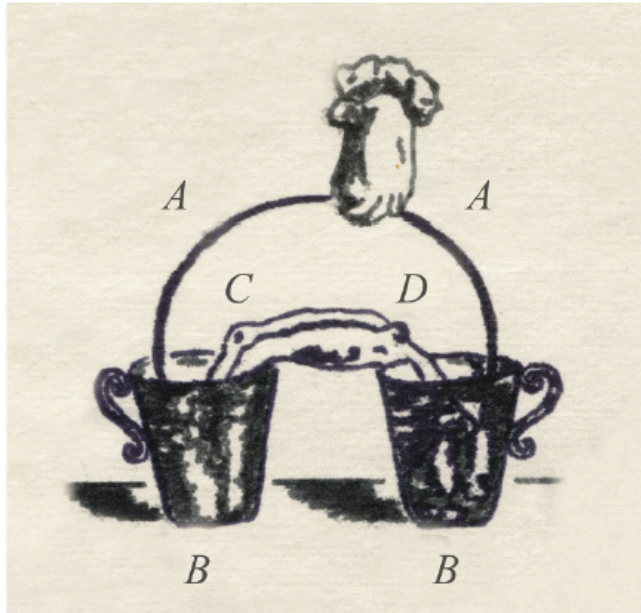
Affiliations | Contributions | Corresponding author

Nature Nanotechnology **10**, 303–307 (2015) | doi:10.1038/nnano.2015.11



Thermoelectric transport

An historical note: Volta and the discovery of thermoelectricity



(see Anatyckuk et al, “On the discovery of thermoelectricity by A. Volta”)

Fig. 3 Schematic of Volta's experiment that resulted in the discovery of thermoelectricity: A – metal (iron) arc; B – glasses with water; C and D – frog parts placed in the glasses with water.

1794-1795: letters from Volta to Vassali. *“I immersed for some half-minute the end of such (iron) arc into boiling water and, without letting it to cool down, returned to experiments with two glasses of cold water. And it was then that the frog in water started contracting...”*

Abram Ioffe (1950s): Doped semiconductors have large thermoelectric effect

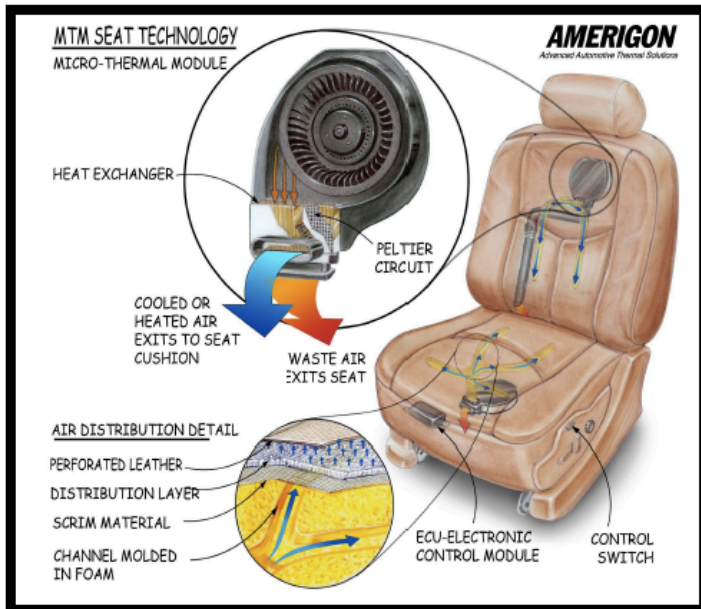
The initial excitement about semiconductors in the 1950s was due to their promise, not in electronics but in refrigeration.

The goal was to build environmental benign solid state home refrigerators and power generators

Thermoelectric (Peltier) refrigerators have poor efficiency compared to compressor-based refrigerators

Niche applications: space missions, medical applications, laboratory equipments, air conditioning in submarines (reliability and quiet operation more important than cost)

car's seats cooler/heater



Use vehicle waste heat to improve fuel economy



Figure 1 | Integrating thermoelectrics into vehicles for improved fuel efficiency. Shown is a BMW 530i concept car with a thermoelectric generator (yellow; and inset) and radiator (red/blue).

Mildred Dresselhaus et al. (Adv. Materials, 2007):

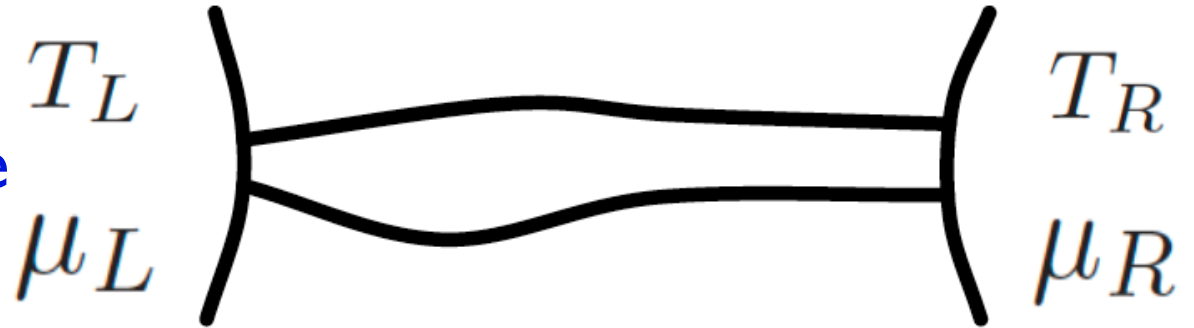
“a newly emerging field of *low-dimensional thermoelectricity*, enabled by *material nanoscience and nanotechnology*...

Thermoelectric phenomena are expected to play an increasingly important role in meeting the energy challenge for the future...”

Small scale thermoelectricity could be relevant for cooling directly on chip, by purely electronic means. *Nanoscale heat management* is crucial to reduce the energy cost in many applications of microelectronics.

Coupled 1D particle and heat transport

Stochastic baths: ideal gases at fixed temperature and chemical potential



$$\begin{cases} J_\rho = L_{\rho\rho}X_1 + L_{\rho q}X_2 \\ J_q = L_{q\rho}X_1 + L_{qq}X_2 \end{cases}$$

Onsager relation:

$$L_{\rho q} = L_{q\rho}$$

Positivity of entropy production:

$$L_{\rho\rho} \geq 0, \quad L_{qq} \geq 0, \quad \det \mathbf{L} \geq 0$$

$$X_1 = \beta \Delta\mu$$

$$X_2 = -\Delta\beta = \Delta T / T^2$$

$$\beta = 1/T$$

$$\Delta\mu = \mu_L - \mu_R$$

$$\Delta\beta = \beta_L - \beta_R$$

$$\Delta T = T_L - T_R$$

(we assume $T_L > T_R$, $\mu_L < \mu_R$)

Onsager and transport coefficients

$$G = \left(\frac{J_\rho}{\Delta\mu/e} \right)_{\Delta T=0} \Rightarrow G = \frac{e^2}{T} L_{\rho\rho}$$

$$\Xi = \left(\frac{J_q}{\Delta T} \right)_{J_\rho=0} \Rightarrow \Xi = \frac{1}{T^2} \frac{\det \mathbf{L}}{L_{\rho\rho}}$$

$$S = - \left(\frac{\Delta\mu/e}{\Delta T} \right)_{J_\rho=0} \Rightarrow S = \frac{1}{eT} \frac{L_{\rho q}}{L_{\rho\rho}}$$

Note that the positivity of entropy production implies that the (isothermal) electric conductance $G > 0$ and the thermal conductance $\Xi > 0$

Maximum efficiency

$$\eta = \frac{\Delta\mu J_\rho}{J_q} = \frac{-TX_1(L_{\rho\rho}X_1 + L_{\rho q}X_2)}{L_{q\rho}X_1 + L_{qq}X_2}$$

Find the maximum of η over X_1 , for fixed X_2 (i.e., over the applied voltage ΔV for fixed temperature difference ΔT)

Maximum achieved for
$$X_1 = \frac{L_{qq}}{L_{q\rho}} \left(-1 + \sqrt{\frac{\det L}{L_{\rho\rho}L_{qq}}} \right) X_2$$

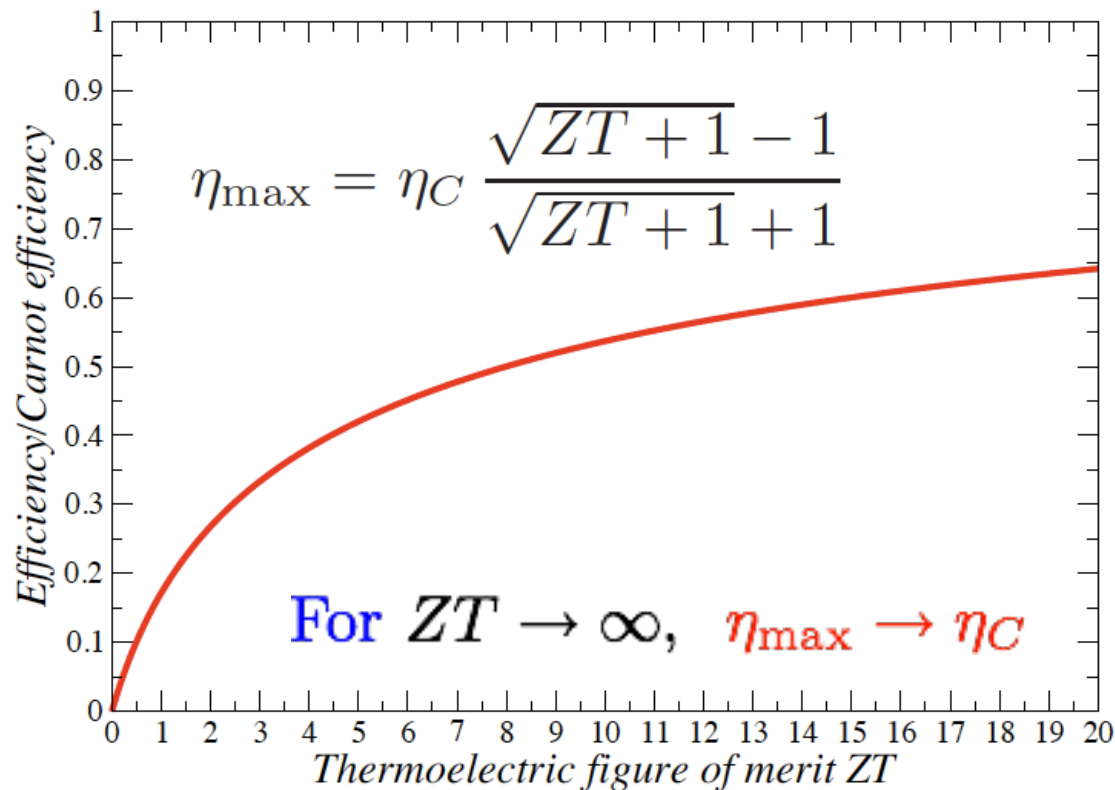
Maximum efficiency (for system with time-reversal symmetry)

$$\eta_{\max} = \eta_C \frac{\sqrt{ZT + 1} - 1}{\sqrt{ZT + 1} + 1}$$

Thermoelectric figure of merit

$$ZT = \frac{L_{q\rho}^2}{\det \mathbf{L}} = \frac{GS^2}{\Xi} T$$

Positivity of entropy production implies $ZT > 0$



Efficiency at maximum power

Output power $\omega = -T X_1 (L_{\rho\rho} X_1 + L_{\rho q} X_2)$

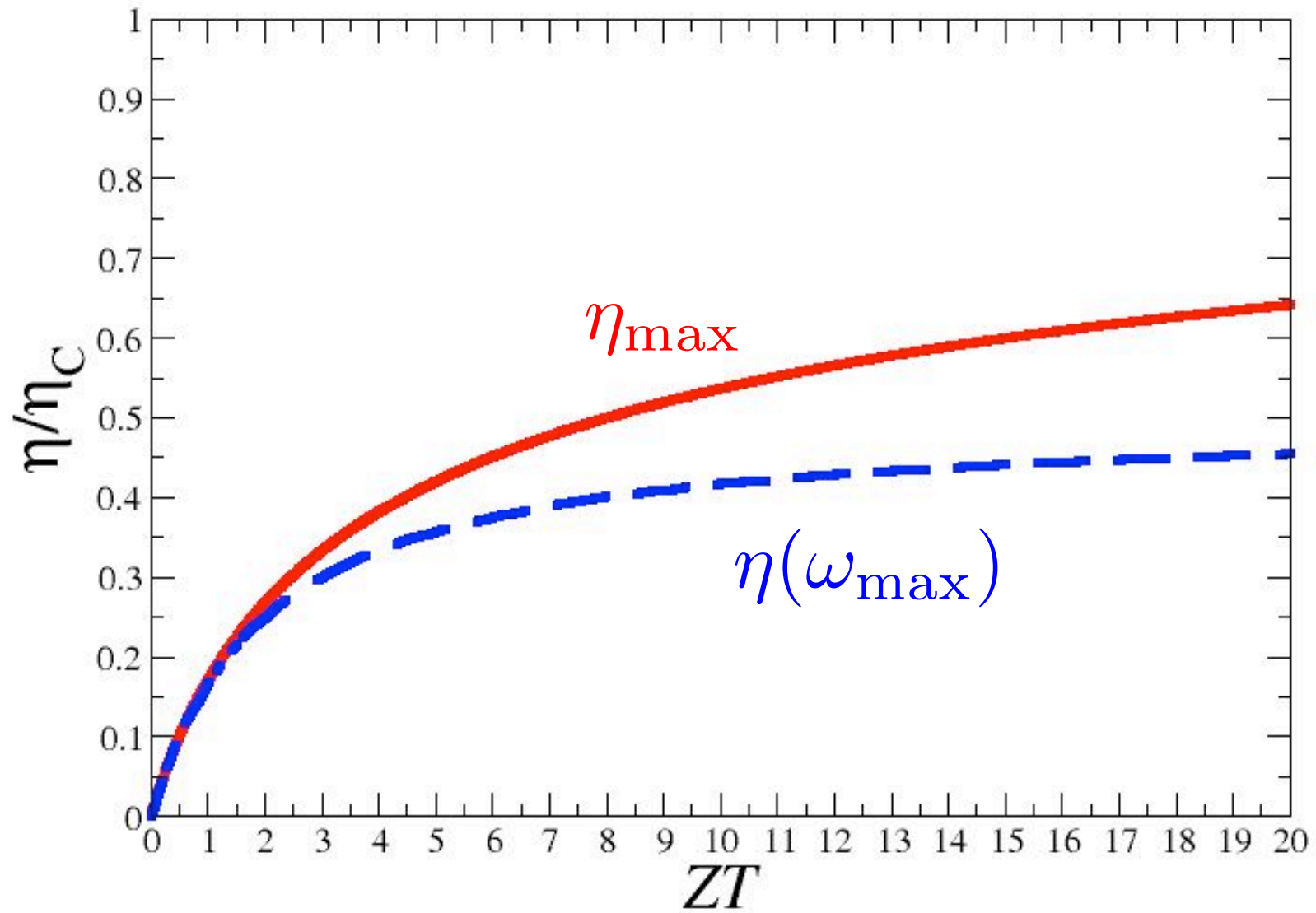
Find the maximum of ω over X_1 , for fixed X_2 (over the applied voltage ΔV for fixed ΔT)

Maximum achieved for $X_1 = -\frac{L_{\rho q}}{2L_{\rho\rho}} X_2$

Efficiency at maximum power

$$\eta(\omega_{\max}) = \frac{\eta_C}{2} \frac{ZT}{ZT + 2} \leq \eta_{CA} \equiv \frac{\eta_C}{2}$$

η_{CA} Curzon-Ahlborn upper bound



Reducing thermal conductivity

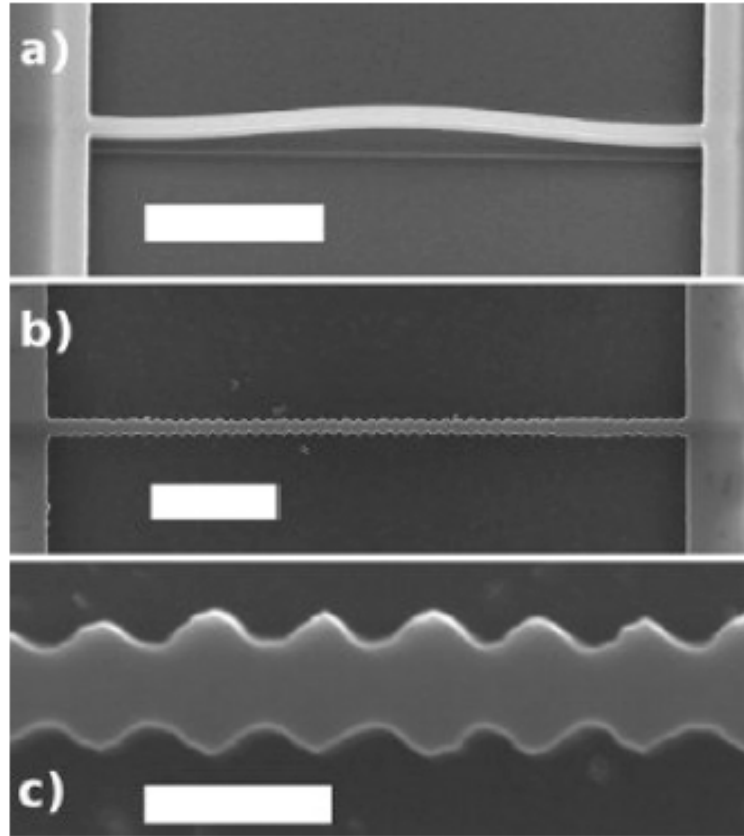


FIG. 1. SEM images of the straight (a) and the corrugated (b) nanowires; (c) corresponds to the top view of the corrugated nanowire. The scale bars correspond to (a) 2 μm, (b) 2 μm, and (c) 300 nm.

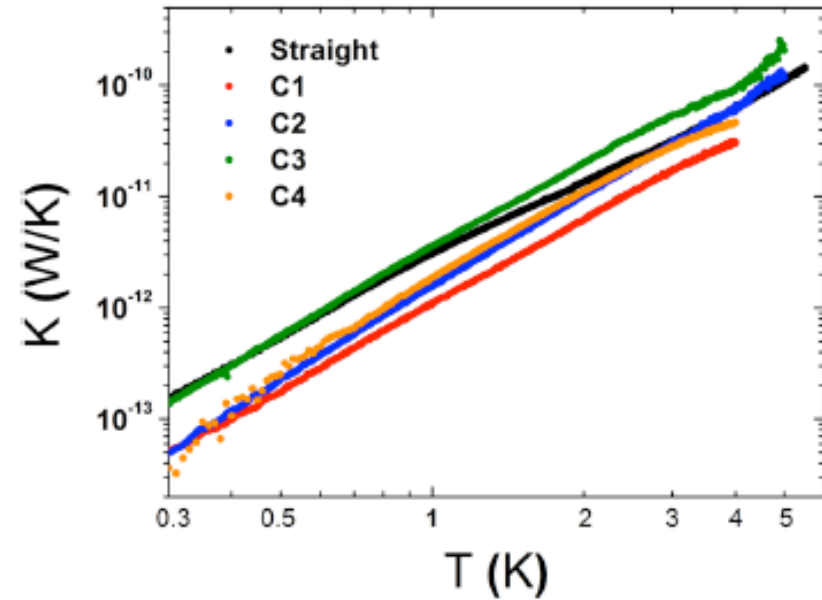


FIG. 2. Thermal conductance versus temperature for a straight nanowire and four corrugated nanowires in the log-log scale.

[Blanc, Rajabpour, Volz, Fournier, Bourgeois, APL **103**, 043109 (2013)]

ZT diverges iff the Onsager matrix is ill-conditioned, that is, the condition number:

$$\text{cond}(\mathbf{L}) \equiv \frac{[\text{Tr}(\mathbf{L})]^2}{\det(\mathbf{L})} \quad \text{diverges}$$

In such case the system is singular (tight-coupling limit):

$$J_q \propto J_\rho$$

(the ratio J_q/J_ρ is independent of the applied voltage and temperature gradients)

Non-interacting systems, Landauer-Büttiker formalism

Charge current

$$J_e = eJ_\rho = \frac{e}{h} \int_{-\infty}^{\infty} dE \tau(E) [f_L(E) - f_R(E)]$$

Heat current from reservoir α

$$J_{q,\alpha} = \frac{1}{h} \int_{-\infty}^{\infty} dE (E - \mu_\alpha) \tau(E) [f_L(E) - f_R(E)]$$

$\tau(E)$ transmission probability for a particle with energy E

$f_\alpha(E)$ Fermi distribution of the particles injected from reservoir α

Thermoelectric efficiency

$$\eta = \frac{[(\mu_R - \mu_L)/e]J_e}{J_{qL}} = \frac{(\mu_R - \mu_L) \int_{-\infty}^{\infty} dE \tau(E) [f_L(E) - f_R(E)]}{\int_{-\infty}^{\infty} dE (E - \mu_L) \tau(E) [f_L(E) - f_R(E)]}$$

If transmission is possible only inside a tiny energy window around $E=E_*$ then

$$\eta = \frac{\mu_L - \mu_R}{E_* - \mu_L}$$

Energy filtering mechanism

In the limit $J_\rho \rightarrow 0$, corresponding to reversible transport

$$\frac{E_\star - \mu_L}{T_L} = \frac{E_\star - \mu_R}{T_R} \Rightarrow E_\star = \frac{\mu_R T_L - \mu_L T_R}{T_L - T_R}$$

$$\eta = \eta_C = 1 - T_R/T_L \quad \text{Carnot efficiency}$$

Carnot efficiency obtained in the limit of reversible transport (zero entropy production) and zero output power

[Mahan and Sofo, PNAS 93, 7436 (1996);
Humphrey et al., PRL 89, 116801 (2002)]

Is energy-filtering necessary to get Carnot efficiency?

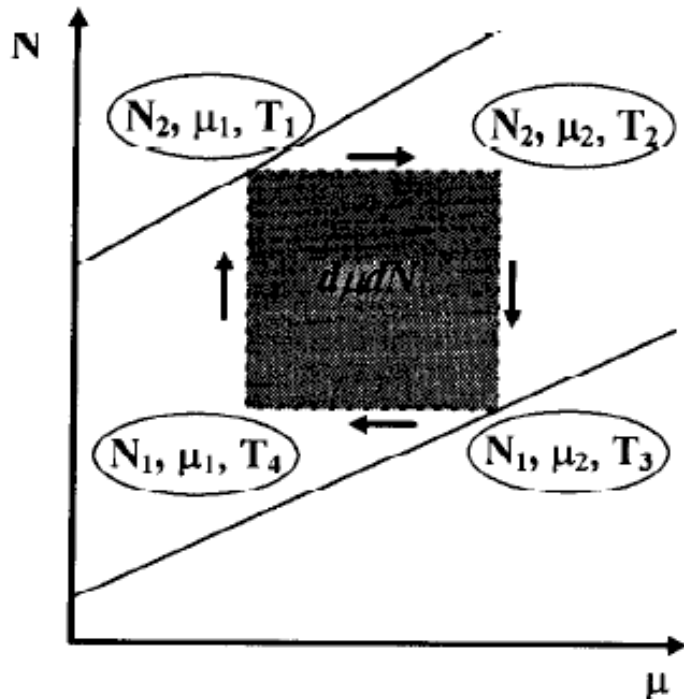
No, for interacting systems with momentum conservation

Short intermezzo: a reason why interactions might be interesting for thermoelectricity

$$1 + ZT = \frac{\kappa'}{\kappa}$$

κ' thermal conductivity at zero electric field

Thermodynamic cycle



$$\frac{\eta}{\eta_C} = \frac{-d\mu dN}{dS dT}$$

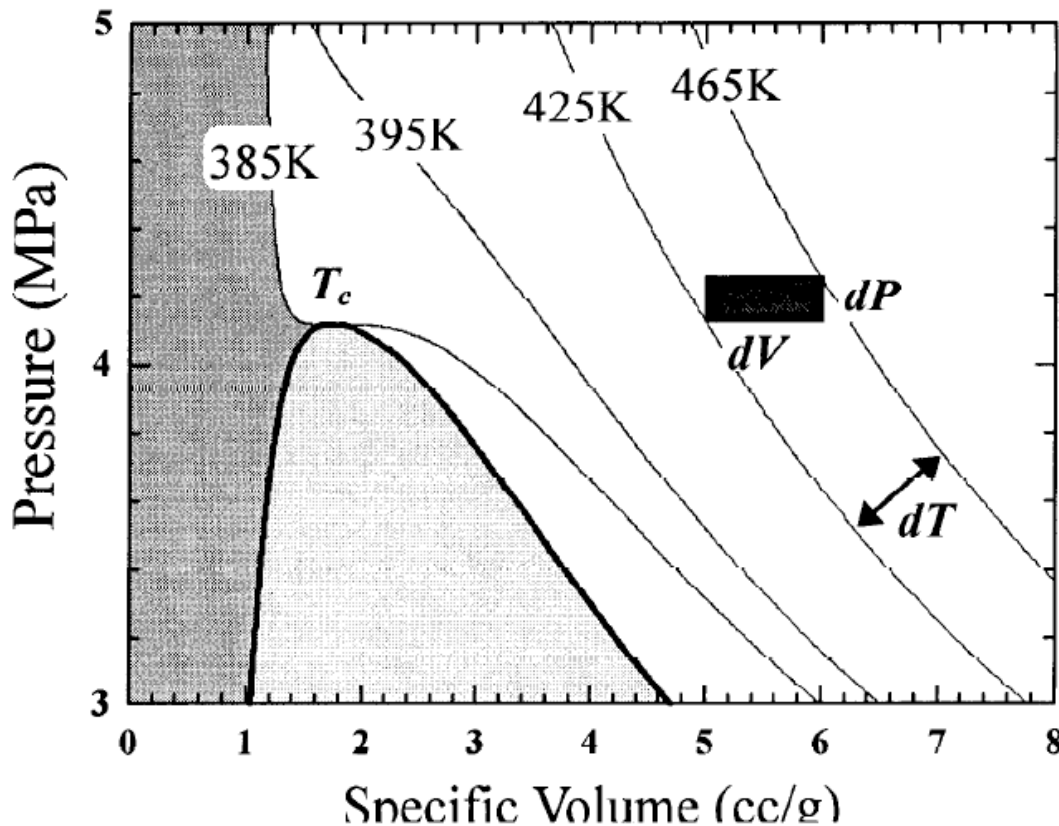
$$1 + Z_{\text{th}} T = \frac{C_{\mu}}{C_N}$$

$$C_{\mu} = \frac{1}{T} \left. \frac{\partial U}{\partial T} \right|_{\mu}, \quad C_N = \frac{1}{T} \left. \frac{\partial U}{\partial T} \right|_N$$

(Vining, MRS Symp. **478**, 3 (1997))

Analogy with a classical gas

$$N \rightarrow V, \quad \mu \rightarrow -p$$



$$\frac{\eta}{\eta_C} = \frac{dpdV}{dSdT}$$

$$1 + Z_{\text{th}}T = \frac{C_p}{C_V}$$

Fig. 5: PV diagram for Freon-12 (CCl_2F_2). The two phase region is light gray and the liquid is the darker gray region to the left. Isotherms are indicated by light lines and a typical $dPdV$ element is indicated by the rectangle.

(Vining, MRS Symp. 478, 3 (1997))

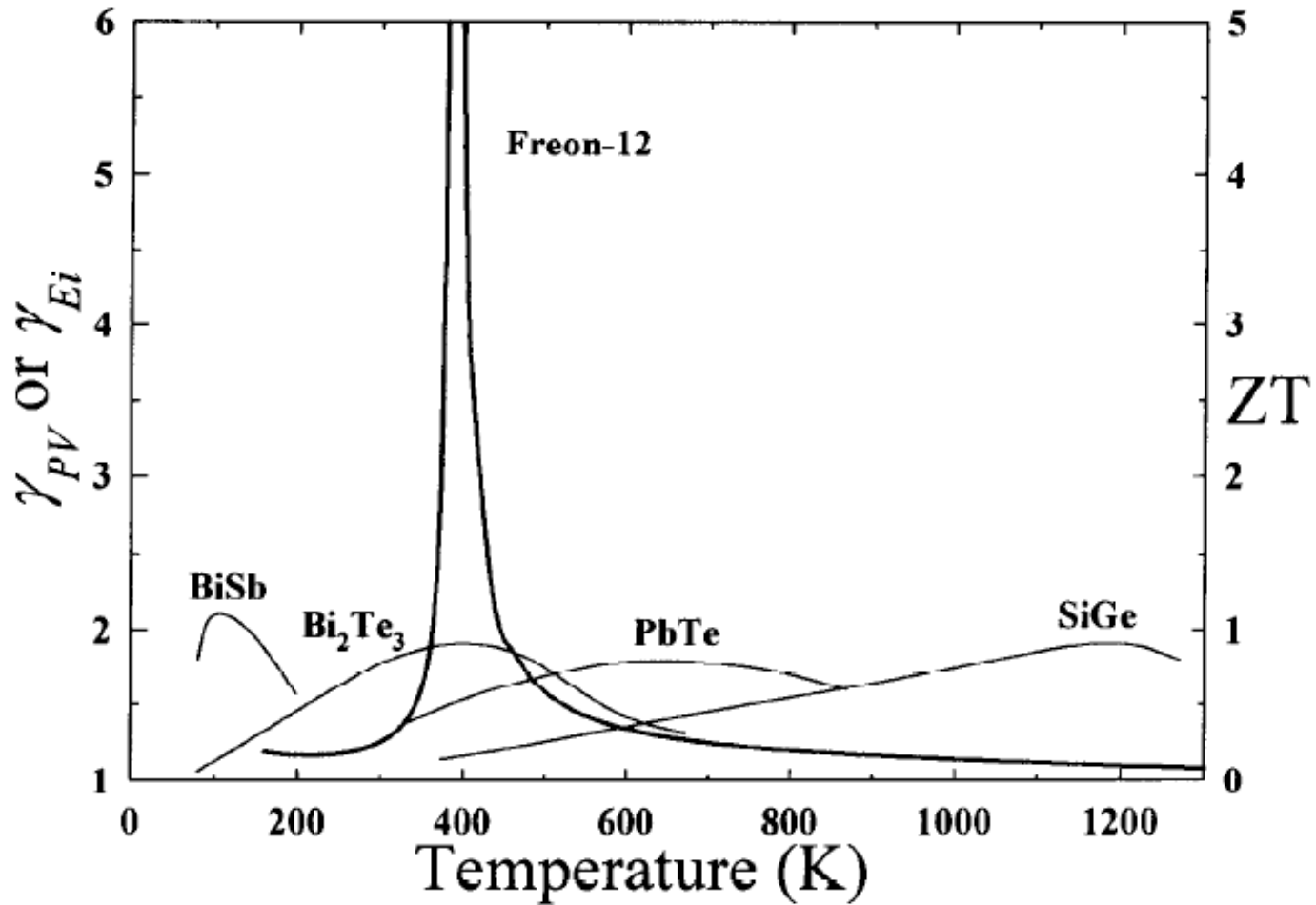
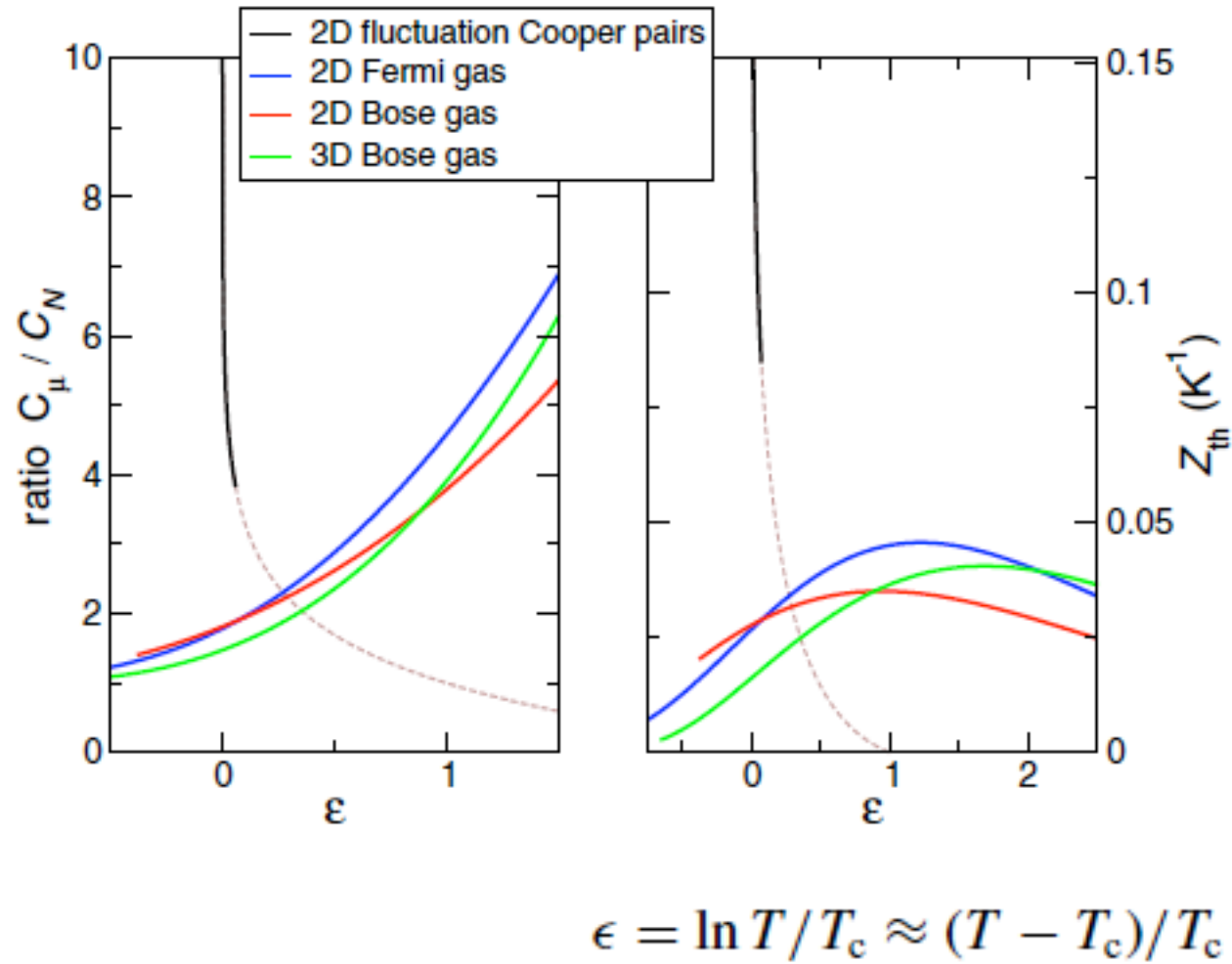


Fig. 4: Specific heat ratios, γ_{PV} for a *PV* system (Freon 12) and thermal conductivity ratios, $\gamma_{Ei}=1+ZT$, for selected *n*-type semiconductor alloys as a function of temperature.

(Vining, MRS Symp. 478, 3 (1997))



(Ouerdane et al., PRB **91**, 100501 (2015))

Interacting systems, Green-Kubo formula

The Green-Kubo formula expresses linear response transport coefficients in terms of dynamic correlation functions of the corresponding current operators, calculated at thermodynamic equilibrium

$$L_{ij} = \lim_{\omega \rightarrow 0} \text{Re} L_{ij}(\omega)$$

$$L_{ij}(\omega) = \lim_{\epsilon \rightarrow 0} \int_0^{\infty} dt e^{-i(\omega - i\epsilon)t} \lim_{\Lambda \rightarrow \infty} \frac{1}{\Lambda} \int_0^{\beta} d\tau \langle J_i J_j(t + i\tau) \rangle_T$$

$$\text{Re} L_{ij}(\omega) = 2\pi \mathcal{D}_{ij} \delta(\omega) + L_{ij}^{\text{reg}}(\omega)$$

Non-zero generalized Drude weights signature of ballistic transport

Conservation laws and thermoelectric efficiency

Suzuki's formula (which generalizes Mazur's inequality) for finite-size Drude weights

$$D_{ij}(\Lambda) \equiv \frac{1}{2\Lambda} \lim_{t \rightarrow \infty} \frac{1}{t} \int_0^t dt' \langle J_i(t') J_j(0) \rangle_T = \frac{1}{2\Lambda} \sum_{n=1}^M \frac{\langle J_i Q_n \rangle_T \langle J_j Q_n \rangle_T}{\langle Q_n^2 \rangle_T}$$

Q_n relevant (i.e., non-orthogonal to charge and thermal currents), mutually orthogonal conserved quantities

$$\mathcal{D}_{ij} = \lim_{t \rightarrow \infty} \lim_{\Lambda \rightarrow \infty} \frac{1}{2\Lambda t} \int_0^t dt' \langle J_i(t') J_j(0) \rangle_T$$

Assuming commutativity of the two limits,

$$\mathcal{D}_{ij} = \lim_{\Lambda \rightarrow \infty} D_{ij}(\Lambda)$$

Momentum-conserving systems

Consider systems with a single relevant constant of motion, notably momentum conservation

Ballistic contribution to $\det(\mathbf{L})$ vanishes as

$$\mathcal{D}_{\rho\rho}\mathcal{D}_{uu} - \mathcal{D}_{\rho u}^2 = 0$$

$$k \propto \frac{\det \mathbf{L}}{L_{\rho\rho}} \propto \Lambda^\alpha, \quad \alpha < 1$$

$$\sigma \propto L_{\rho\rho} \propto \Lambda \quad ZT = \frac{\sigma S^2}{\kappa} T \propto \Lambda^{1-\alpha} \rightarrow \infty \text{ when } \Lambda \rightarrow \infty$$

$$S \propto \frac{L_{\rho q}}{L_{\rho\rho}} \propto \Lambda^0$$

(G.B., G. Casati, J. Wang, PRL 110, 070604 (2013))

For systems with more than a single relevant constant of motion, for instance for **integrable systems**, due to the Schwarz inequality

$$D_{\rho\rho}D_{uu} - D_{\rho u}^2 = \|\mathbf{x}_\rho\|^2 \|\mathbf{x}_u\|^2 - \langle \mathbf{x}_\rho, \mathbf{x}_u \rangle^2 \geq 0$$

$$\mathbf{x}_i = (x_{i1}, \dots, x_{iM}) = \frac{1}{2\Lambda} \left(\frac{\langle J_i Q_1 \rangle_T}{\sqrt{\langle Q_1^2 \rangle_T}}, \dots, \frac{\langle J_i Q_M \rangle_T}{\sqrt{\langle Q_M^2 \rangle_T}} \right)$$

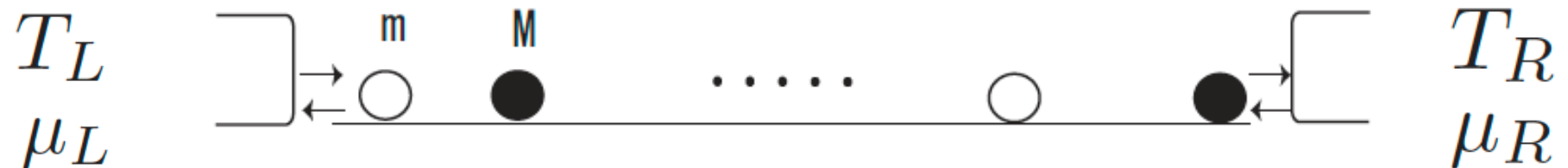
$$\langle \mathbf{x}_\rho, \mathbf{x}_u \rangle = \sum_{k=1}^M x_{\rho k} x_{uk}$$

Equality arises only in the exceptional case when the two vectors are parallel; in general

$$\det \mathbf{L} \propto L^2, \quad \kappa \propto \Lambda, \quad ZT \propto \Lambda^0$$

Example: 1D interacting classical gas

Consider a **one dimensional gas** of hard-point elastically colliding particles with **unequal masses: m, M**



For $M = m$ (integrable model)

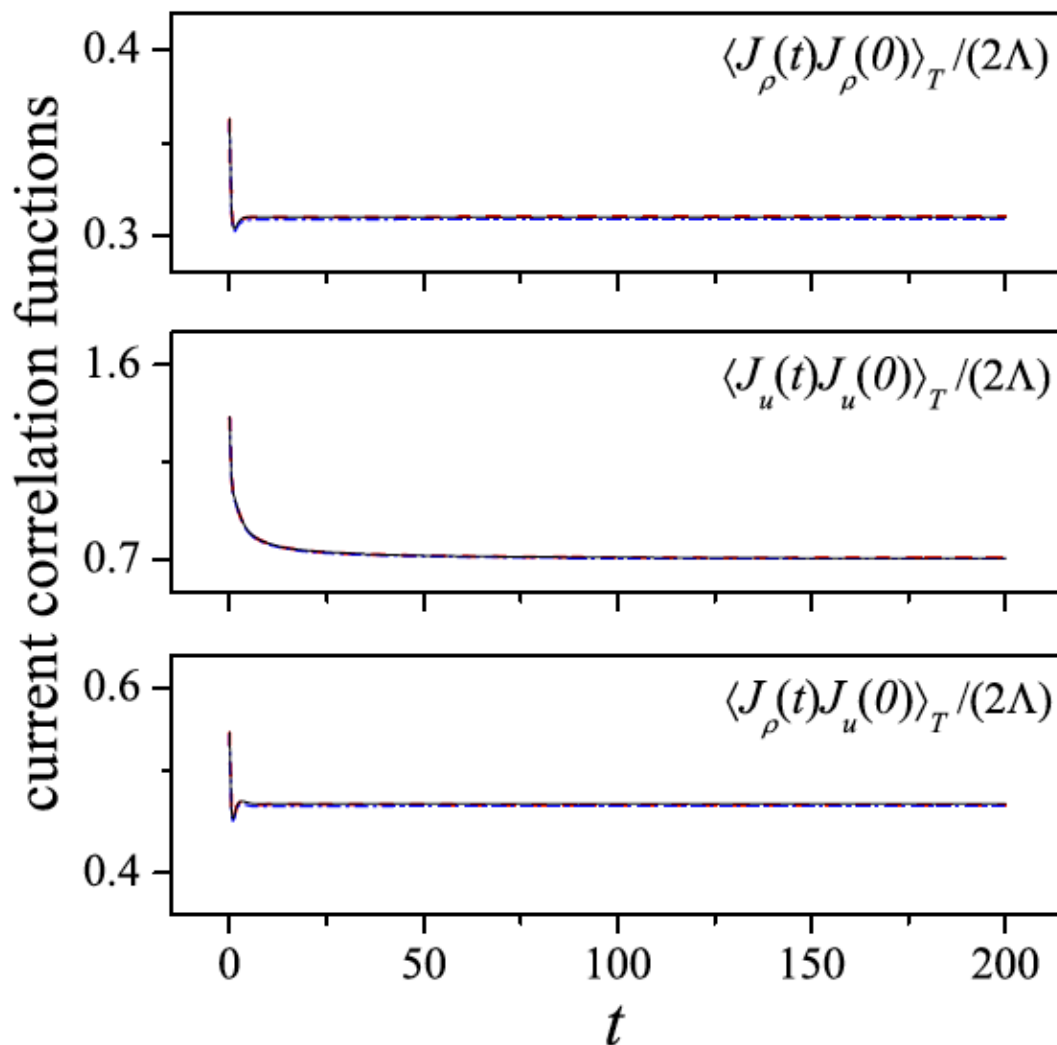
$$J_u = T_L \gamma_L - T_R \gamma_R \quad (J_u = J_q + \mu J_\rho)$$

$$J_\rho = \gamma_L - \gamma_R. \quad ZT = 1 \text{ (at } \mu = 0)$$

$$\gamma_\alpha = \frac{1}{h\beta_\alpha} e^{\beta_\alpha \mu_\alpha} \quad \text{injection rates}$$

For $M \neq m$ ZT depends on the system size

Non-decaying correlation functions



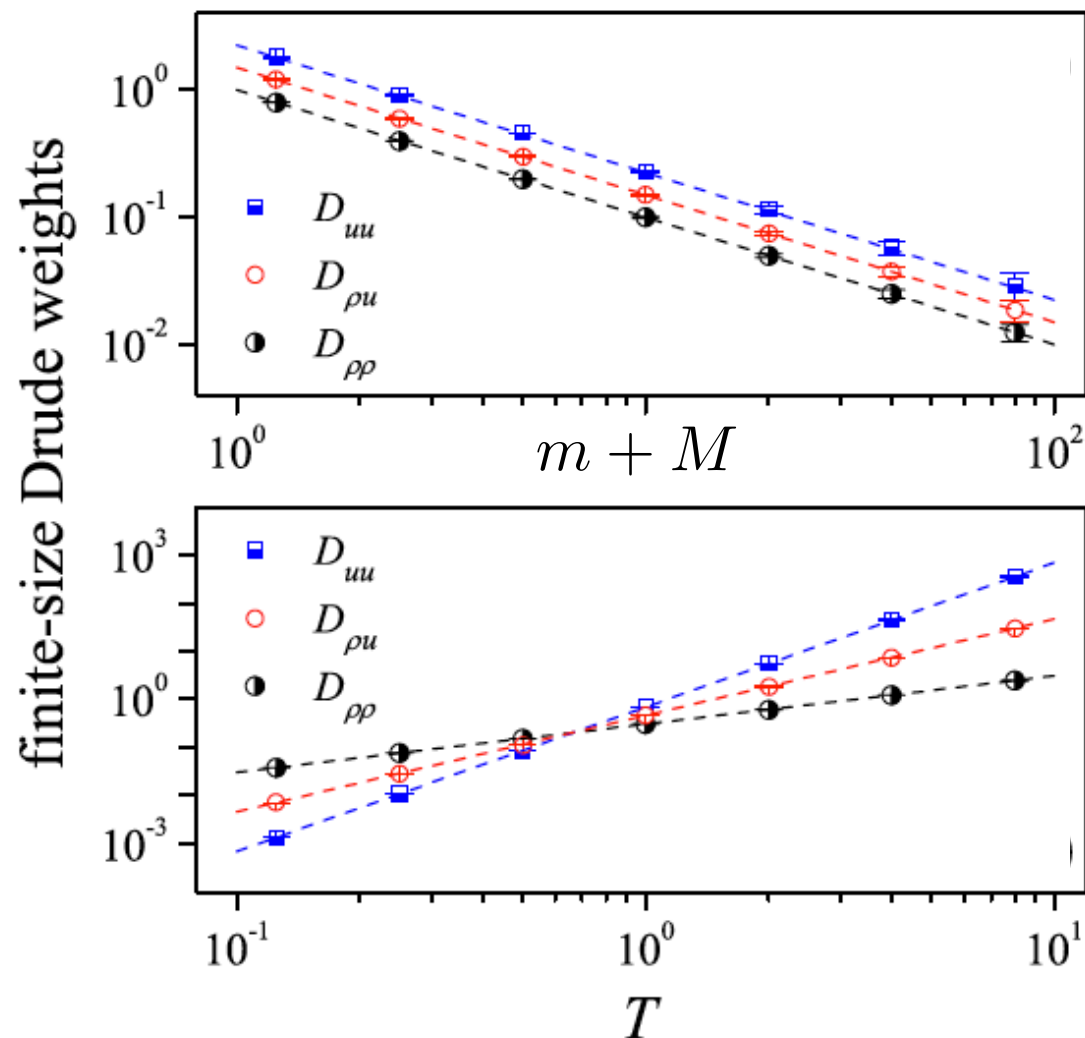
$\Lambda = 256$ (red dashed curve), 512 (blue dash-dotted curve),
and 1024 (black solid curve)

Finite-size Drude weights: analytical results vs. numerics

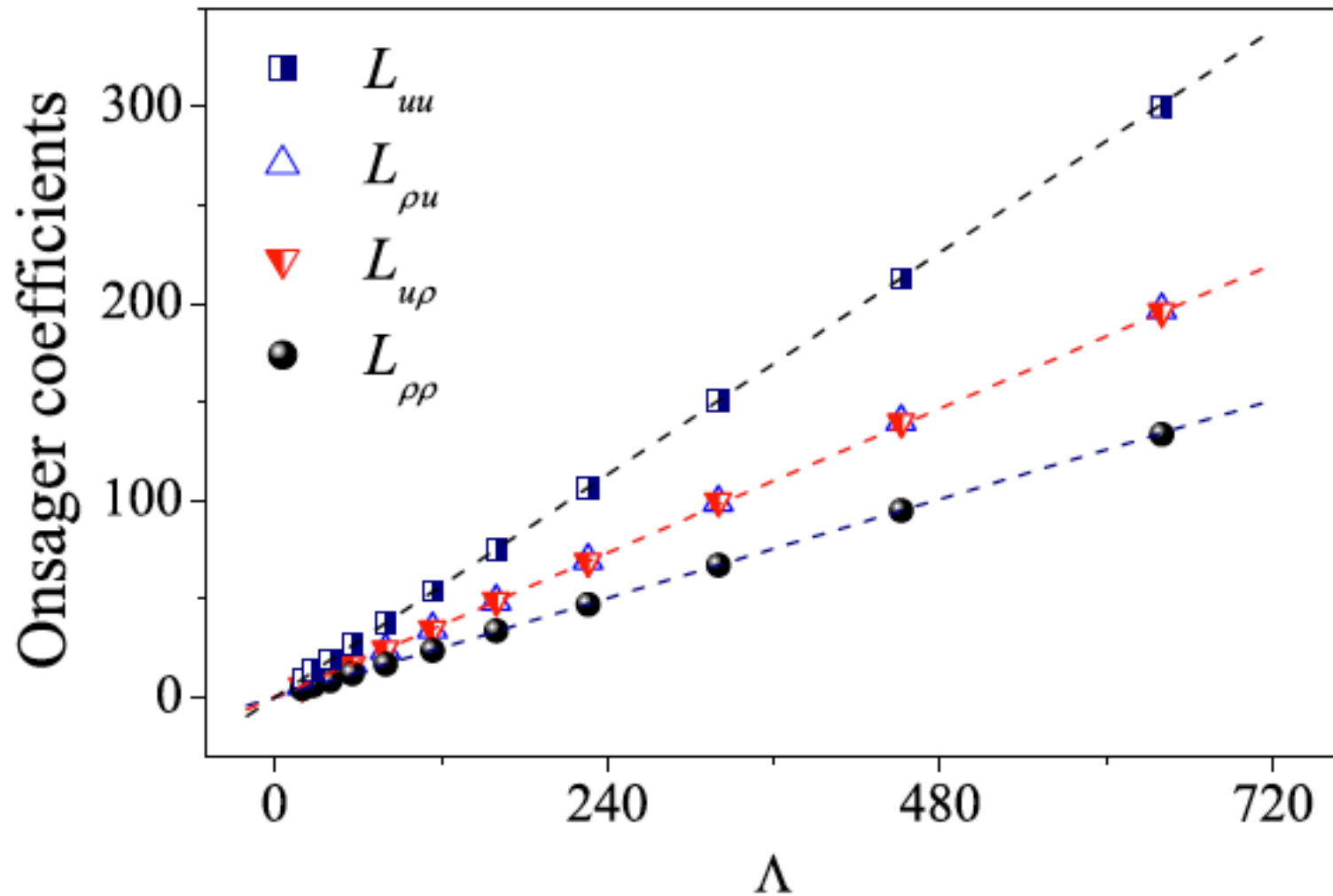
$$D_{\rho\rho}(\Lambda) = \frac{TN^2}{2\Lambda(mN_1 + MN_2)},$$

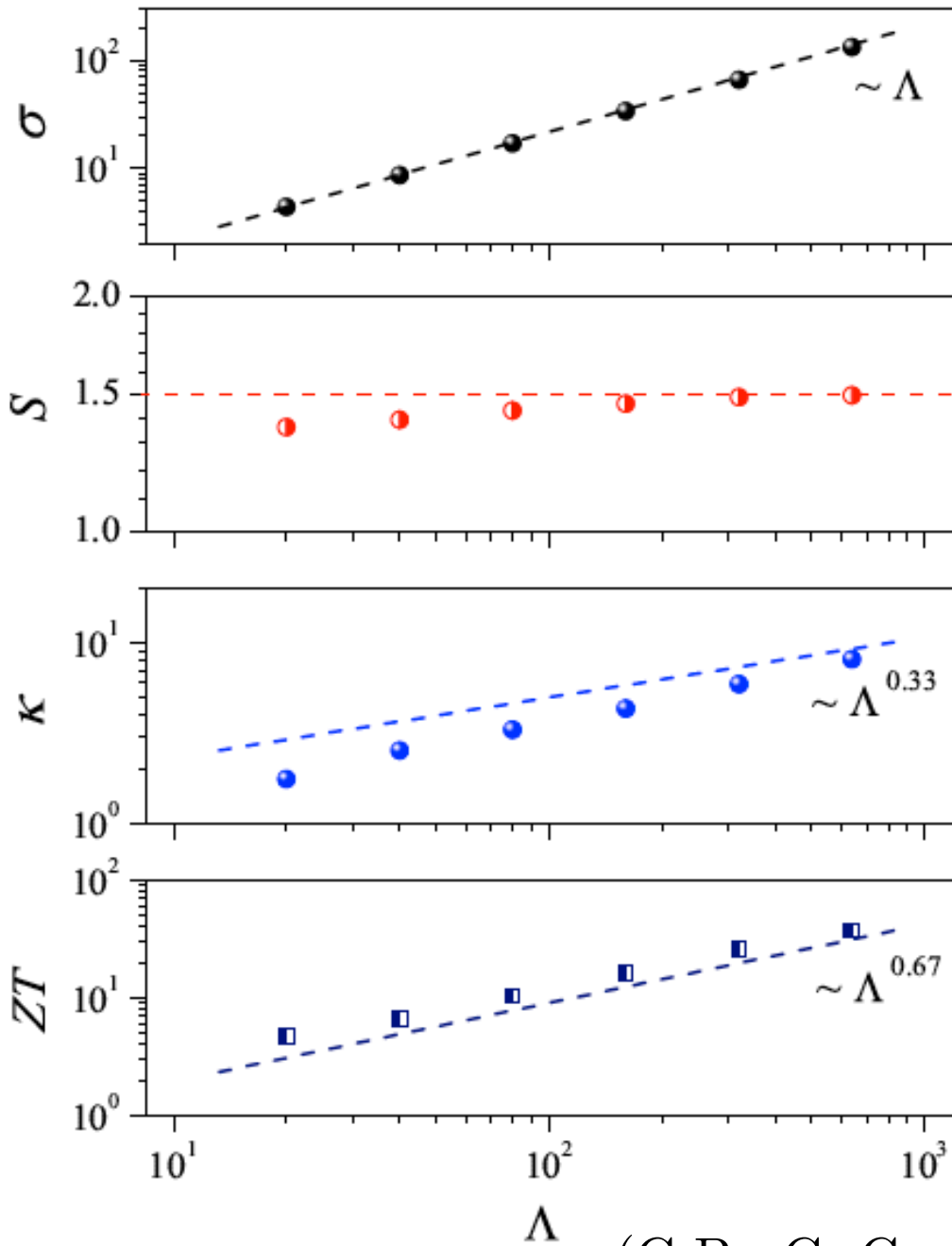
$$D_{uu}(\Lambda) = \frac{9T^3 N^2}{8\Lambda(mN_1 + MN_2)},$$

$$D_{\rho u}(\Lambda) = \frac{3T^2 N^2}{4\Lambda(mN_1 + MN_2)}.$$



Ballistic behavior of Onsager coefficients





Anomalous thermal transport

$$ZT = \frac{\sigma S^2}{k} T$$

ZT diverges
increasing the systems size

(G.B., G. Casati, J. Wang, PRL 110, 070604 (2013))

Energy-filtering mechanism?

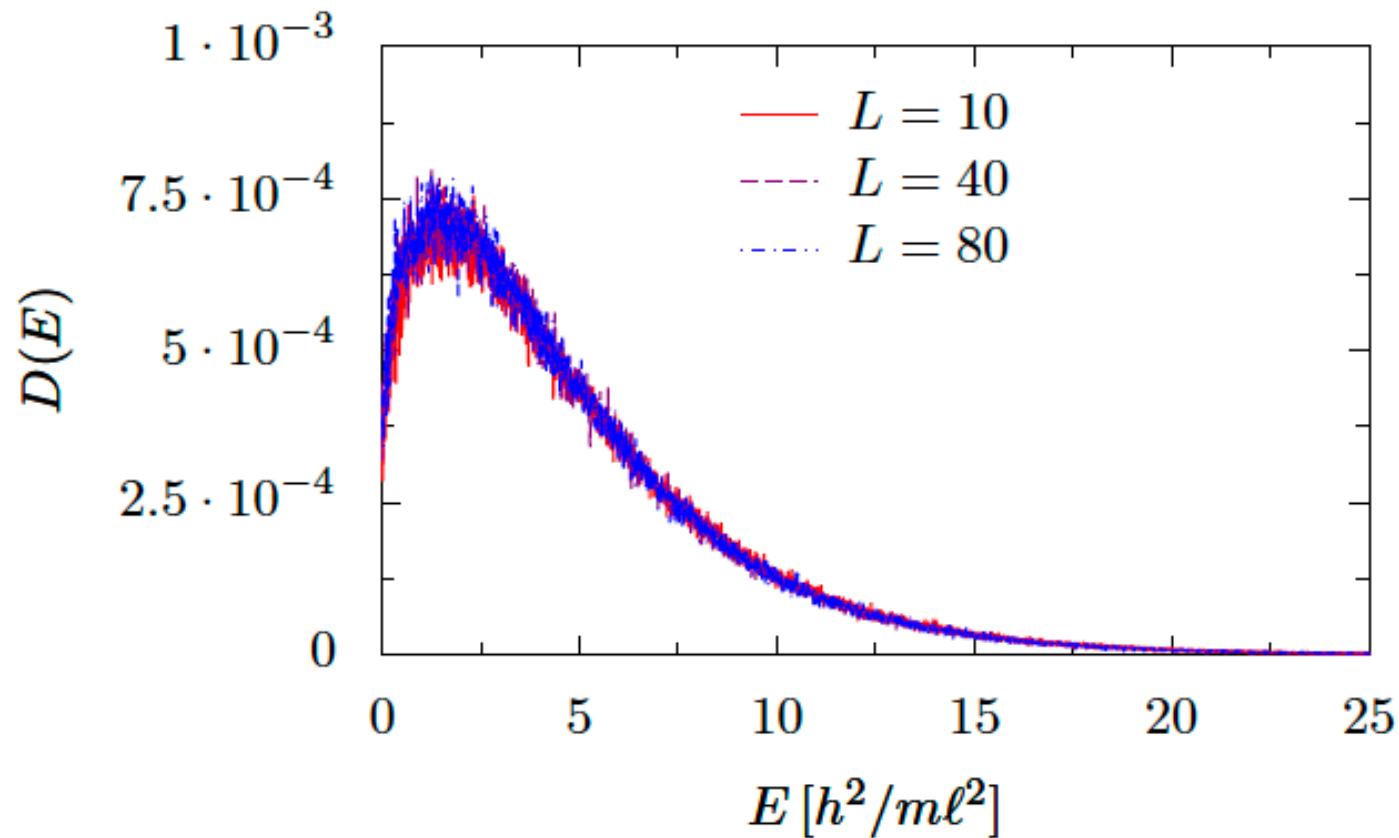
At a given position \mathbf{x} compute:

$$J_\rho = \int_0^\infty dE D(E)$$

$D(E) \equiv D_L(E) - D_R(E)$ “transmission function”

$D_L(E)$ Density of particles crossing \mathbf{x} from left

$D_R(E)$ Density of particles crossing \mathbf{x} from right

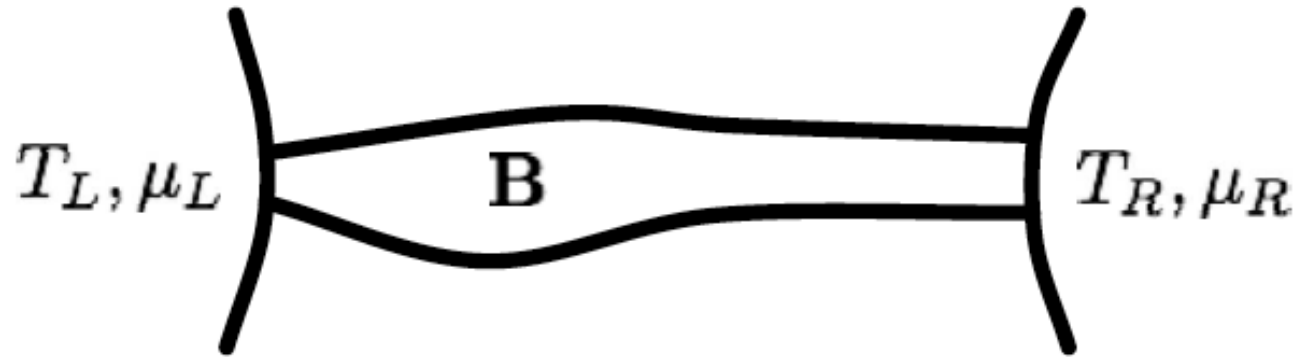


There is no sign of narrowing of $D(E)$ with increasing the system size L

A mechanism for increasing ZT **different from energy filtering is needed**

(K. Saito, G.B., G. Casati, Chem. Phys. 375, 508 (2010))

And when time-reversal is broken?



$$\begin{cases} J_\rho(\mathbf{B}) = L_{\rho\rho}(\mathbf{B})X_1 + L_{\rho q}(\mathbf{B})X_2 \\ J_q(\mathbf{B}) = L_{q\rho}(\mathbf{B})X_1 + L_{qq}(\mathbf{B})X_2 \end{cases} \quad \begin{aligned} X_1 &= \beta\Delta\mu \\ X_2 &= -\Delta\beta = \Delta T/T^2 \\ \beta &= 1/T \end{aligned}$$

\mathbf{B} applied magnetic field or any parameter breaking time-reversibility such as the Coriolis force, etc.

$$\Delta\mu = \mu_L - \mu_R$$

$$\Delta\beta = \beta_L - \beta_R$$

$$\Delta T = T_L - T_R$$

(we assume $T_L > T_R$, $\mu_L < \mu_R$)

Constraints from thermodynamics

POSITIVITY OF THE ENTROPY PRODUCTION:

$$\dot{S} = J_\rho X_1 + J_q X_2 \geq 0 \quad \Rightarrow \quad \begin{cases} L_{\rho\rho} \geq 0, \\ L_{qq} \geq 0, \\ L_{\rho\rho}L_{qq} - \frac{1}{4}(L_{\rho q} + L_{q\rho})^2 \geq 0 \end{cases}$$

ONSAGER-CASIMIR RELATIONS:

$$L_{ij}(\mathbf{B}) = L_{ji}(-\mathbf{B}) \quad \Rightarrow \quad \begin{aligned} \sigma(\mathbf{B}) &= \sigma(-\mathbf{B}) \\ \kappa(\mathbf{B}) &= \kappa(-\mathbf{B}) \end{aligned}$$

in general, $S(\mathbf{B}) \neq S(-\mathbf{B})$

Both maximum efficiency and efficiency at maximum power depend on two parameters

$$x \equiv \frac{L_{\rho q}}{L_{q\rho}} = \frac{S(\mathbf{B})}{S(-\mathbf{B})},$$

$$y = \frac{L_{\rho q}L_{q\rho}}{\det\mathbf{L}} = \frac{\sigma(\mathbf{B})S(\mathbf{B})S(-\mathbf{B})}{\kappa(\mathbf{B})} T.$$

$$\eta(\omega_{\max}) = \frac{\eta_C}{2} \frac{xy}{2+y} \quad \eta_{\max} = \eta_C x \frac{\sqrt{y+1}-1}{\sqrt{y+1}+1}$$

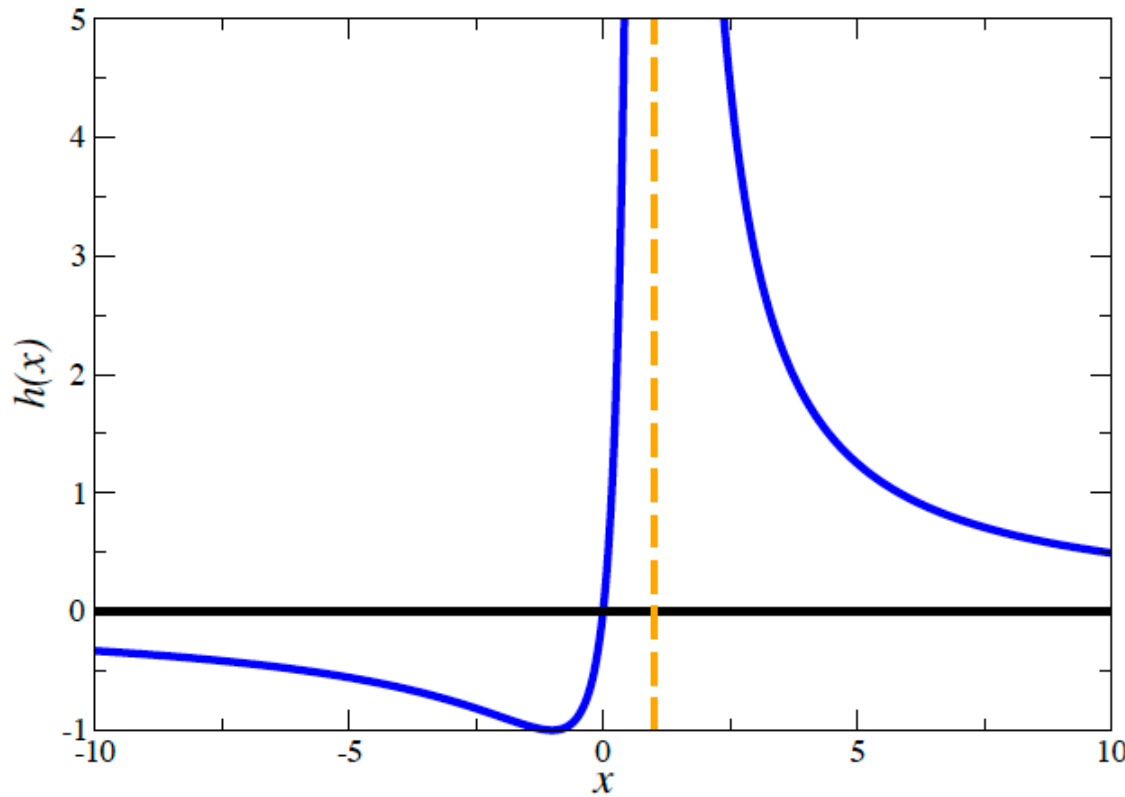
At $B = 0$ there is time-reversibility and:

asymmetry parameter $x = 1$

the efficiency only depends on $y(x = 1) = ZT$

$$L_{\rho\rho}L_{qq} - \frac{1}{4}(L_{\rho q} + L_{q\rho})^2 \geq 0 \Rightarrow$$

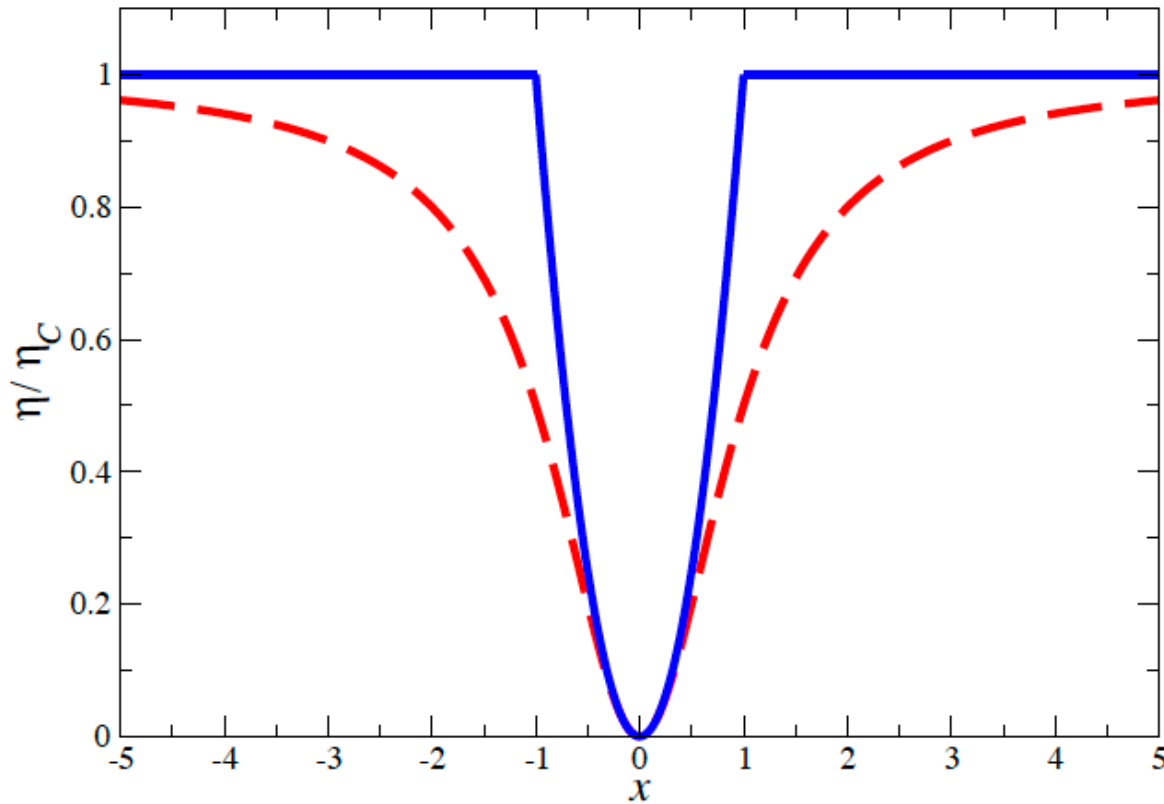
$$\begin{cases} h(x) \leq y \leq 0 & \text{if } x < 0 \\ 0 \leq y \leq h(x) & \text{if } x > 0 \end{cases}$$



$$h(x) = 4x/(x-1)^2$$

maximum efficiencies
achieved for $y = h(x)$

$$\bar{\eta}(P_{\max}) = \eta_C \frac{x^2}{x^2 + 1}, \quad \bar{\eta}_{\max} = \begin{cases} \eta_C x^2 & \text{if } |x| \leq 1, \\ \eta_C & \text{if } |x| \geq 1. \end{cases}$$



The CA limit can be overcome within linear response

When $|x|$ is large the figure of merit y required to get Carnot efficiency becomes small

Carnot efficiency could be obtained far from the tight-coupling condition

(G.B., K. Saito, G. Casati, PRL **106**, 230602 (2011))

OUTPUT POWER AT MAXIMUM EFFICIENCY

$$\omega(\eta_M) = \frac{\eta_M}{4} \frac{|L_{\rho q}^2 - L_{q\rho}^2|}{L_{\rho\rho}} X_2$$

When time-reversibility is broken, within linear response is it possible to have simultaneously Carnot efficiency and non-zero power.

Terms of higher order in the entropy production, beyond linear response, will generally be non-zero. However, irrespective how close we are to the Carnot efficiency, we can find small enough forces such that the linear theory holds.

Reversible part of the currents

$$J_i^{\text{rev}} \equiv \frac{L_{ij} - L_{ji}}{2} X_j, \quad i = \rho, q$$

$$J_i^{\text{irr}} \equiv L_{ii} X_i + \frac{L_{ij} + L_{ji}}{2} X_j$$

The reversible part of the currents do not contribute to entropy production

$$\dot{S} = J_\rho X_1 + J_q X_2 = J_\rho^{\text{irr}} X_1 + J_q^{\text{irr}} X_2$$

Possibility of dissipationless transport?

(K. Brandner, K. Saito, U. Seifert, PRL **110**, 070603 (2013))

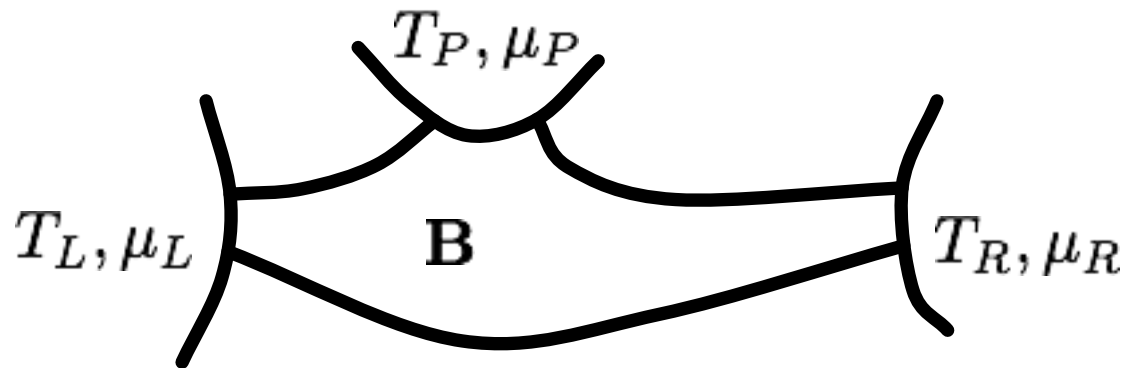
How to obtain asymmetry in the Seebeck coefficient?

For non-interacting systems, due to the symmetry properties of the scattering matrix $\Rightarrow S(\mathbf{B}) = S(-\mathbf{B})$

This symmetry does not apply when electron-phonon and electron-electron interactions are taken into account

Let us consider the case of partially coherent transport, with inelastic processes simulated by “conceptual probes” (Buttiker, 1988).

Non-interacting three-terminal model



P probe reservoir

$$T_L = T + \Delta T, \quad T_R = T$$

$$\mu_L = \mu + \Delta\mu, \quad \mu_R = \mu$$

$$T_P = T + \Delta T_P$$

$$\mu_P = \mu + \Delta\mu$$

Charge and energy conservation:

$$\sum_k J_{\rho,k} = 0,$$

$$\sum_k J_{E,k} = 0, \quad (k = L, R, P)$$

Entropy production (linear response):

$$\dot{S} = {}^t\mathbf{J}\mathbf{X} = \sum_{i=1}^4 J_i X_i,$$

$${}^t\mathbf{J} = (eJ_{\rho,L}, J_{q,L}, eJ_{\rho,P}, J_{q,P})$$

$${}^t\mathbf{X} = \left(\frac{\Delta\mu}{eT}, \frac{\Delta T}{T^2}, \frac{\Delta\mu_P}{eT}, \frac{\Delta T_P}{T^2} \right)$$

$$(J_{q,k} = J_{E,k} - \mu J_{\rho,k})$$

Three-terminal Onsager matrix

Equation connecting fluxes and thermodynamic forces:

$$\mathbf{J} = \mathbf{L}\mathbf{X}$$

\mathbf{L} is a 4×4 Onsager matrix

In block-matrix form:

$$\begin{pmatrix} \mathbf{J}_\alpha \\ \mathbf{J}_\beta \end{pmatrix} = \begin{pmatrix} \mathbf{L}_{\alpha\alpha} & \mathbf{L}_{\alpha\beta} \\ \mathbf{L}_{\beta\alpha} & \mathbf{L}_{\beta\beta} \end{pmatrix} \begin{pmatrix} \mathbf{X}_\alpha \\ \mathbf{X}_\beta \end{pmatrix}$$

Zero-particle and heat current condition through the probe terminal:

$$\mathbf{J}_\beta = (J_3, J_4) = 0 \quad \Rightarrow \quad \mathbf{X}_\beta = -\mathbf{L}_{\beta\beta}^{-1} \mathbf{L}_{\beta\alpha} \mathbf{X}_\alpha$$

Two-terminal Onsager matrix for partially coherent transport

Reduction to 2x2 Onsager matrix when the third terminal is a probe terminal mimicking phase-breaking.

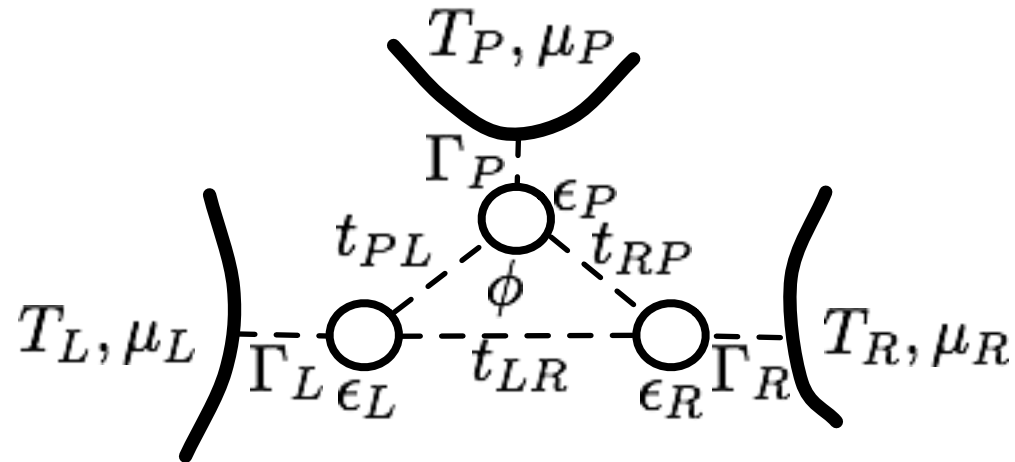
$$\mathbf{J}_\alpha = \mathbf{L}_{\alpha\alpha}' \mathbf{X}_\alpha, \quad \mathbf{L}_{\alpha\alpha}' \equiv (\mathbf{L}_{\alpha\alpha} - \mathbf{L}_{\alpha\beta} \mathbf{L}_{\beta\beta}^{-1} \mathbf{L}_{\beta\alpha})$$

$$\begin{pmatrix} J_1 \\ J_2 \end{pmatrix} = \begin{pmatrix} L'_{11} & L'_{12} \\ L'_{21} & L'_{22} \end{pmatrix} \begin{pmatrix} X_1 \\ X_2 \end{pmatrix}$$

\mathbf{L}' is the two-terminal Onsager matrix for partially coherent transport

The Seebeck coefficient is not bounded to be symmetric in \mathbf{B} (for asymmetric structures)

Illustrative three-dot example

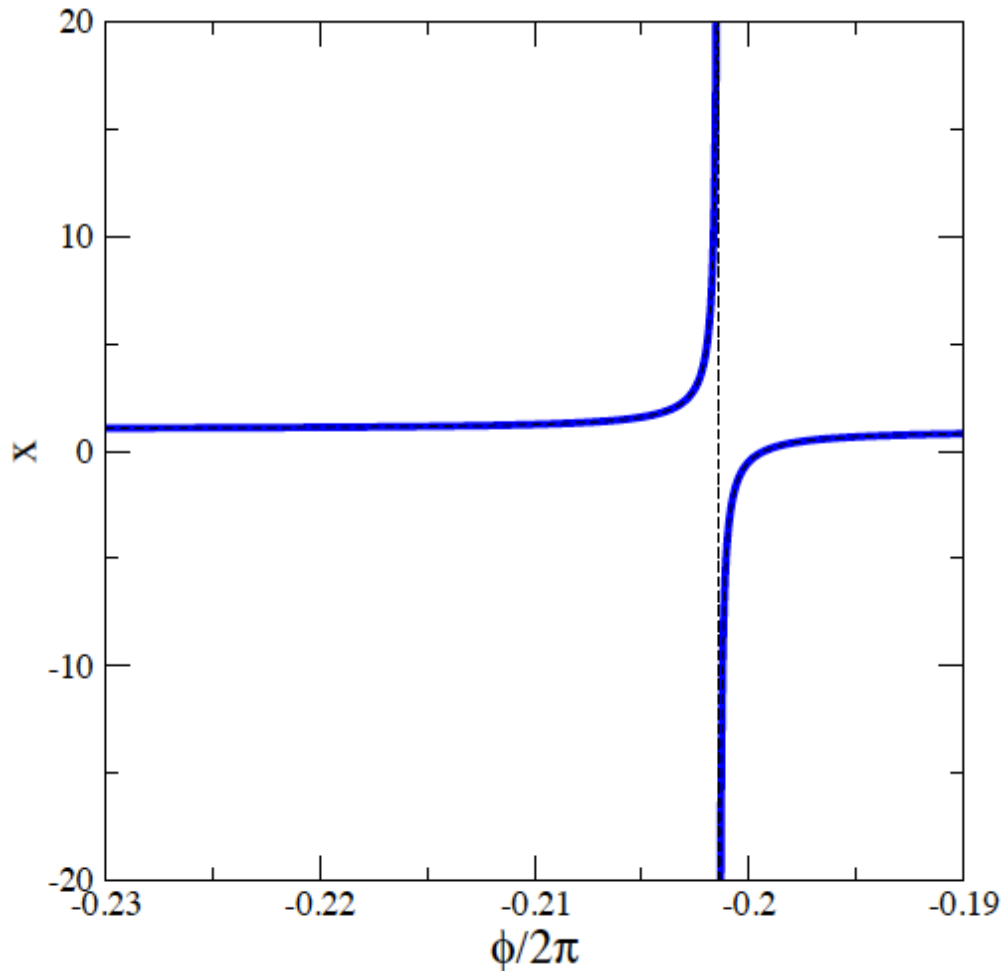


$$H_S = \sum_k \epsilon_k c_k^\dagger c_k + (t_{LR} c_R^\dagger c_L e^{i\phi/3} + t_{RP} c_P^\dagger c_R e^{i\phi/3} + t_{PL} c_L^\dagger c_P e^{i\phi/3} + \text{H.c.})$$

Asymmetric structure, e.g.. $\epsilon_L \neq \epsilon_R$

First-principle exact calculation within the Landauer-Büttiker multi-terminal approach

Asymmetric Seebeck coefficient



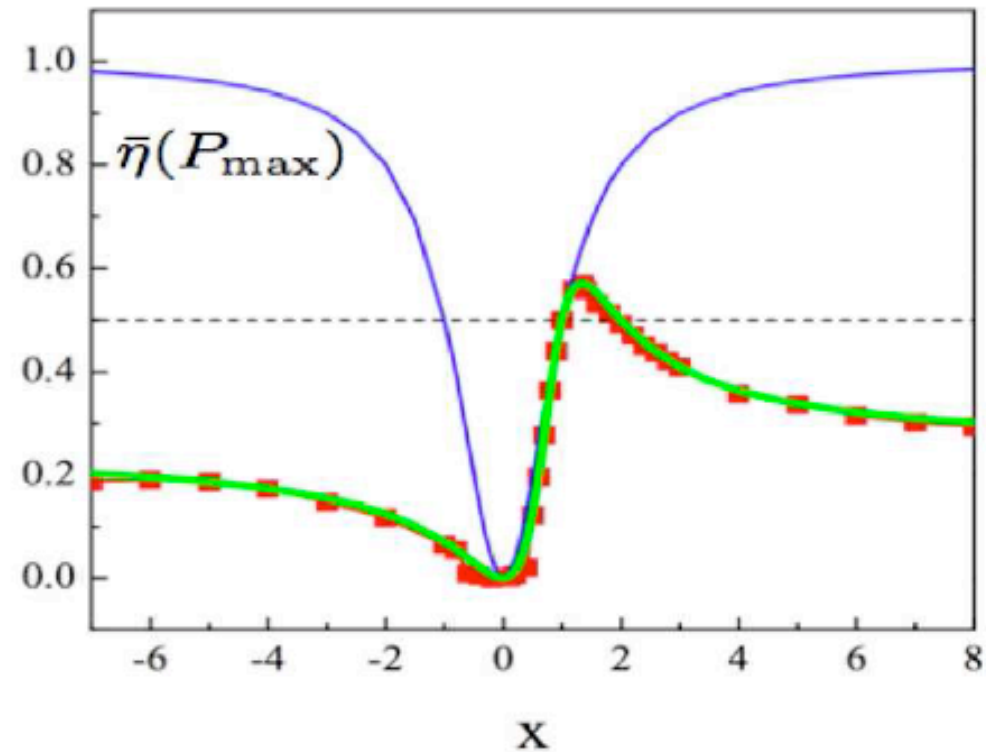
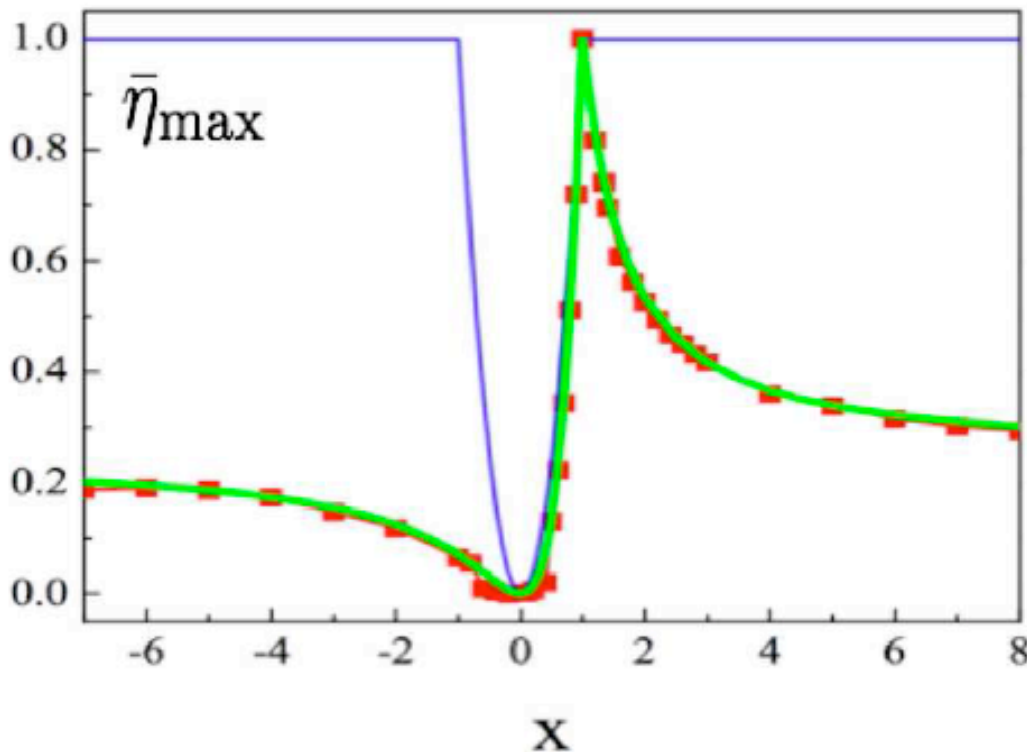
$$x(\phi) = \frac{L'_{12}(\phi)}{L'_{21}(\phi)} = \frac{S(\phi)}{S(-\phi)} \neq 1$$

(K. Saito, G. B., G. Casati, T. Prosen, PRB **84**, 201306(R) (2011))
(see also D. Sánchez, L. Serra, PRB **84**, 201307(R) (2011))

Bounds beyond the second law of thermodynamics from the unitarity of S-matrix

Bounds obtained for non-interacting 3-terminal transport

(K. Brandner, K. Saito, U. Seifert, PRL **110**, 070603 (2013))



(Numerics: V. Balachandran, G. B.,
G. Casati, PRB **87**, 165419 (2013));

$$\eta(\omega_{\max}) = \frac{4}{7} \eta_C \quad \text{at} \quad x = \frac{4}{3}$$

Magnetic thermal switch (n-terminal setup)

$$\mathbf{J}(\mathbf{B}) = \mathbf{J}^{(r)}(\mathbf{B}) + \mathbf{J}^{(i)}(\mathbf{B})$$

$$\mathbf{J}^{(r)} \equiv \frac{\mathbf{L}(\mathbf{B}) - \mathbf{L}^T(\mathbf{B})}{2} \mathbf{X}, \quad \mathbf{J}^{(i)} \equiv \frac{\mathbf{L}(\mathbf{B}) + \mathbf{L}^T(\mathbf{B})}{2} \mathbf{X}$$

$$\mathbf{J}^{(r)}(\mathbf{B}) = -\mathbf{J}^{(r)}(-\mathbf{B}) \quad \mathbf{J}^{(i)}(\mathbf{B}) = \mathbf{J}^{(i)}(-\mathbf{B})$$

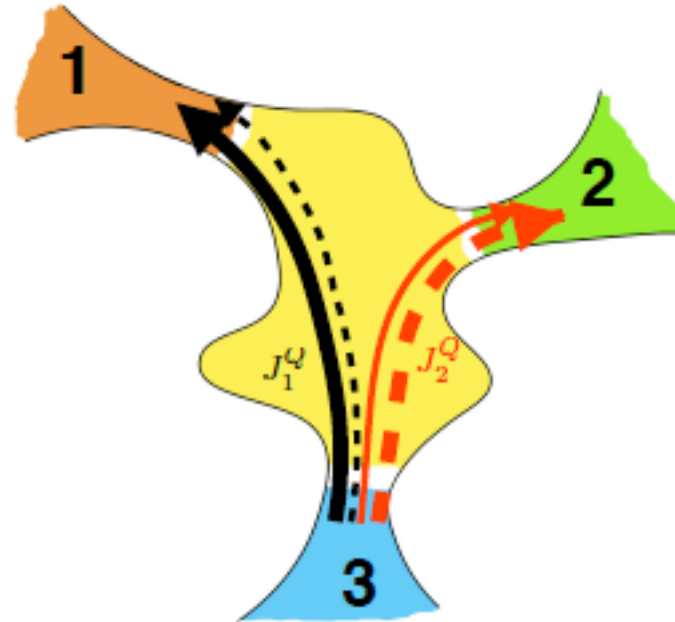
Set voltages (for fixed thermal affinities) to obtain conditions on the currents from a subset K of the n terminals:

$$J_k^Q(-\mathbf{B}) = \sum_{k'=1}^{n-1} x_{kk'}^{(\text{target})} J_{k'}^Q(\mathbf{B}), \quad \forall k \in K$$

(R. Bosisio, S. Valentini, F. Mazza, G.B., V. Giovannetti, R. Fazio, F. Taddei, PRB **91**, 205420 (2015))

Heat current multiplier:

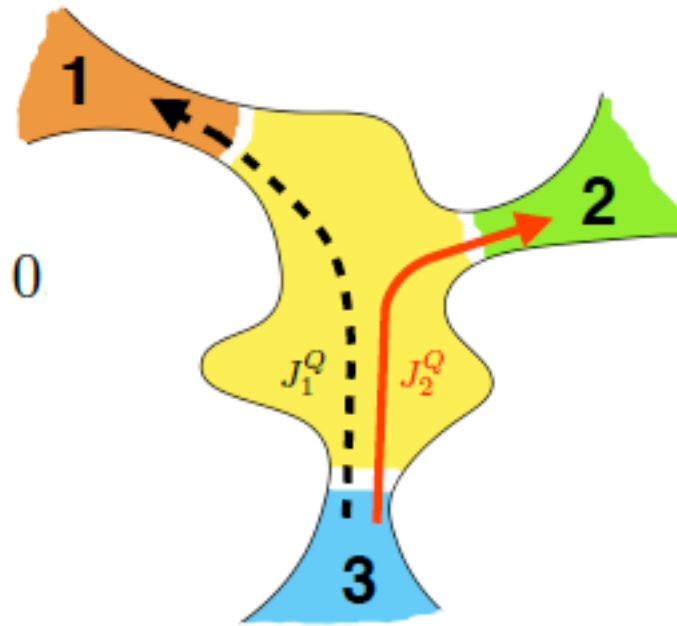
$$J_k^Q(-\mathbf{B}) = x_k J_k^Q(\mathbf{B})$$



Heat path selector:

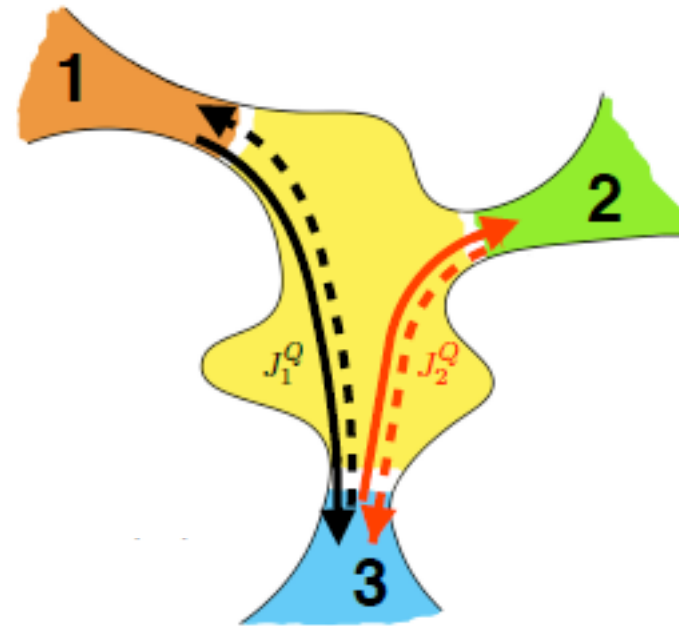
$$J_k^Q(-\mathbf{B}) = J_k^{Q(r)}(-\mathbf{B}) + J_k^{Q(i)}(-\mathbf{B}) = 0$$

$$J_k^Q(\mathbf{B}) = J_k^{Q(r)}(\mathbf{B}) + J_k^{Q(i)}(\mathbf{B}) \neq 0$$



Fully reversible heat:

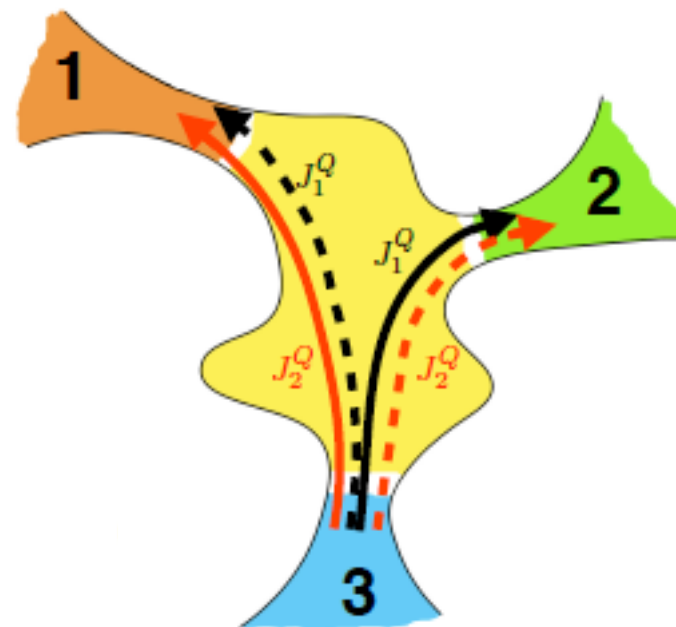
$$J_k^{Q(i)} = 0$$



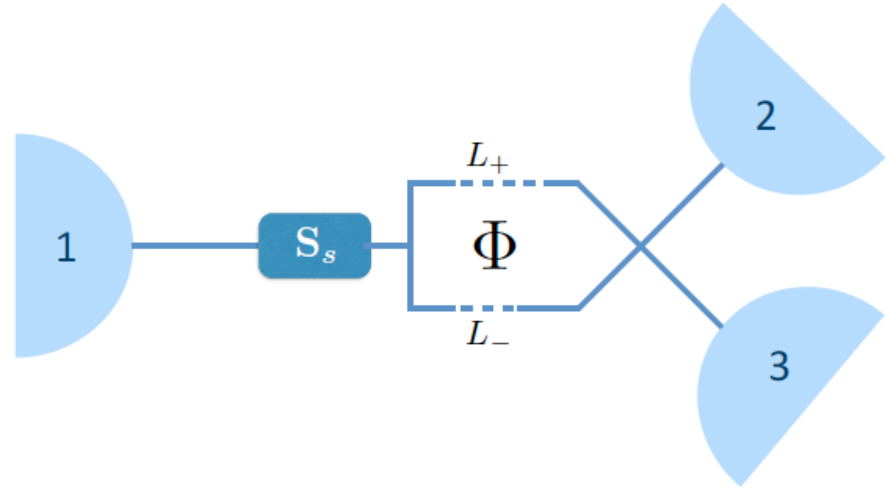
Heat current swap:

$$J_k^Q(\mathbf{B}) = J_{k'}^Q(-\mathbf{B})$$

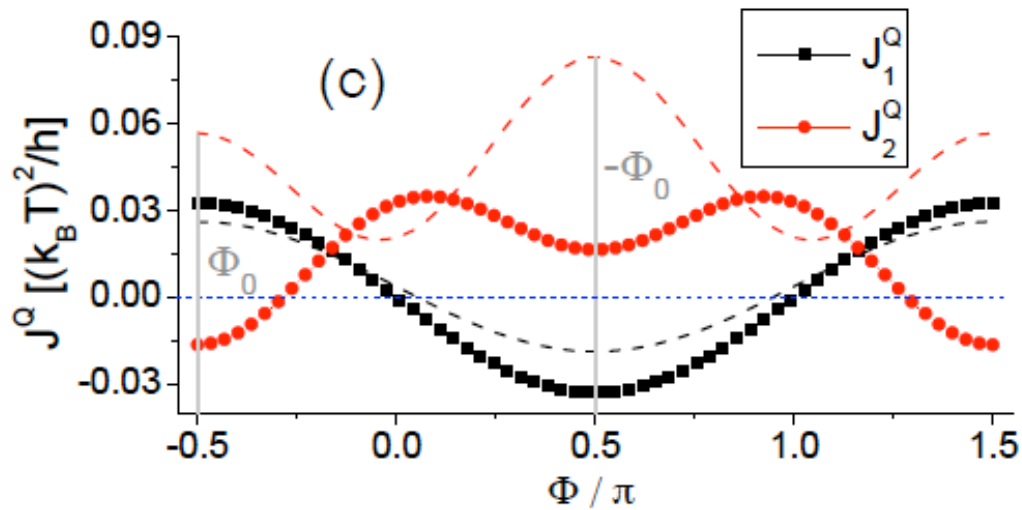
$$J_{k'}^Q(\mathbf{B}) = J_k^Q(-\mathbf{B})$$



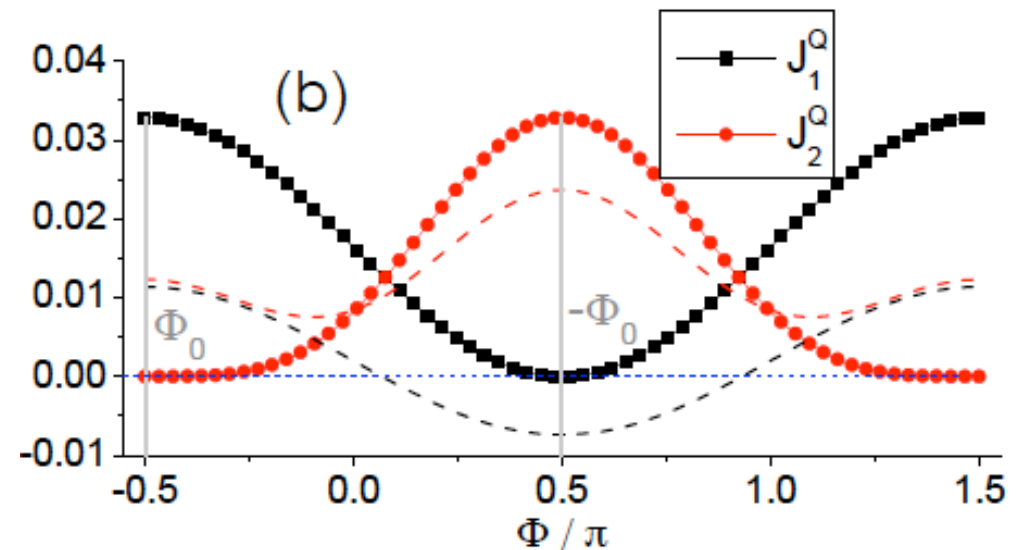
Example: interferometer model



Fully reversible heat:

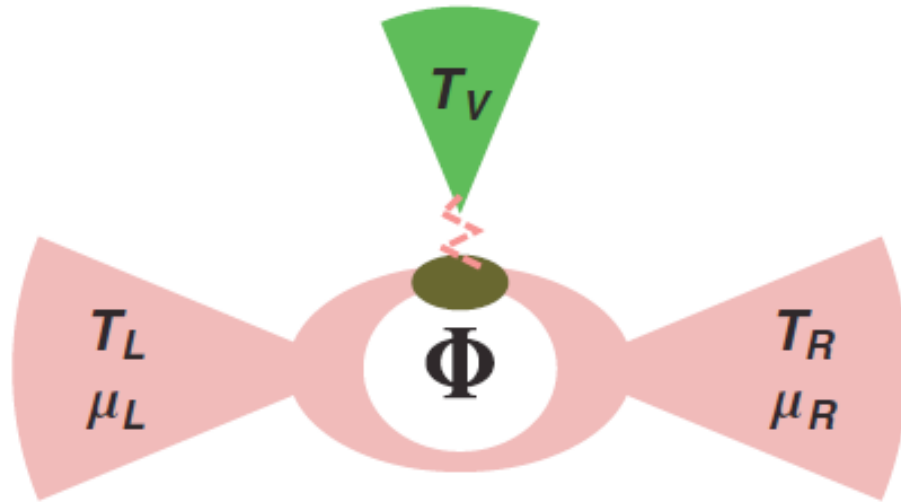


Heat path selector:



(R. Bosisio, S. Valentini, F. Mazza, G.B., V. Giovannetti, R. Fazio, F. Taddei,
PRB **91**, 205420 (2015))

Switch also applicable to phononic currents

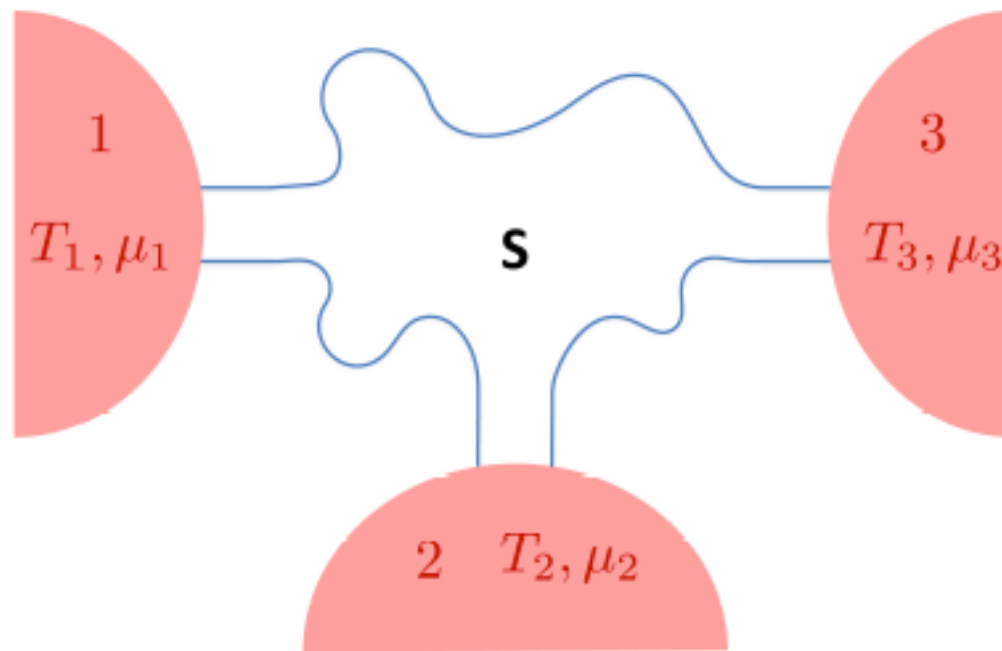


(O. Entin-Wolman, A. Aharony,
PRB **85**, 085401 (2012))

Due to **electron-phonon coupling** the thermal current from the bosonic terminal has a reversible component

Multi-terminal thermoelectricity

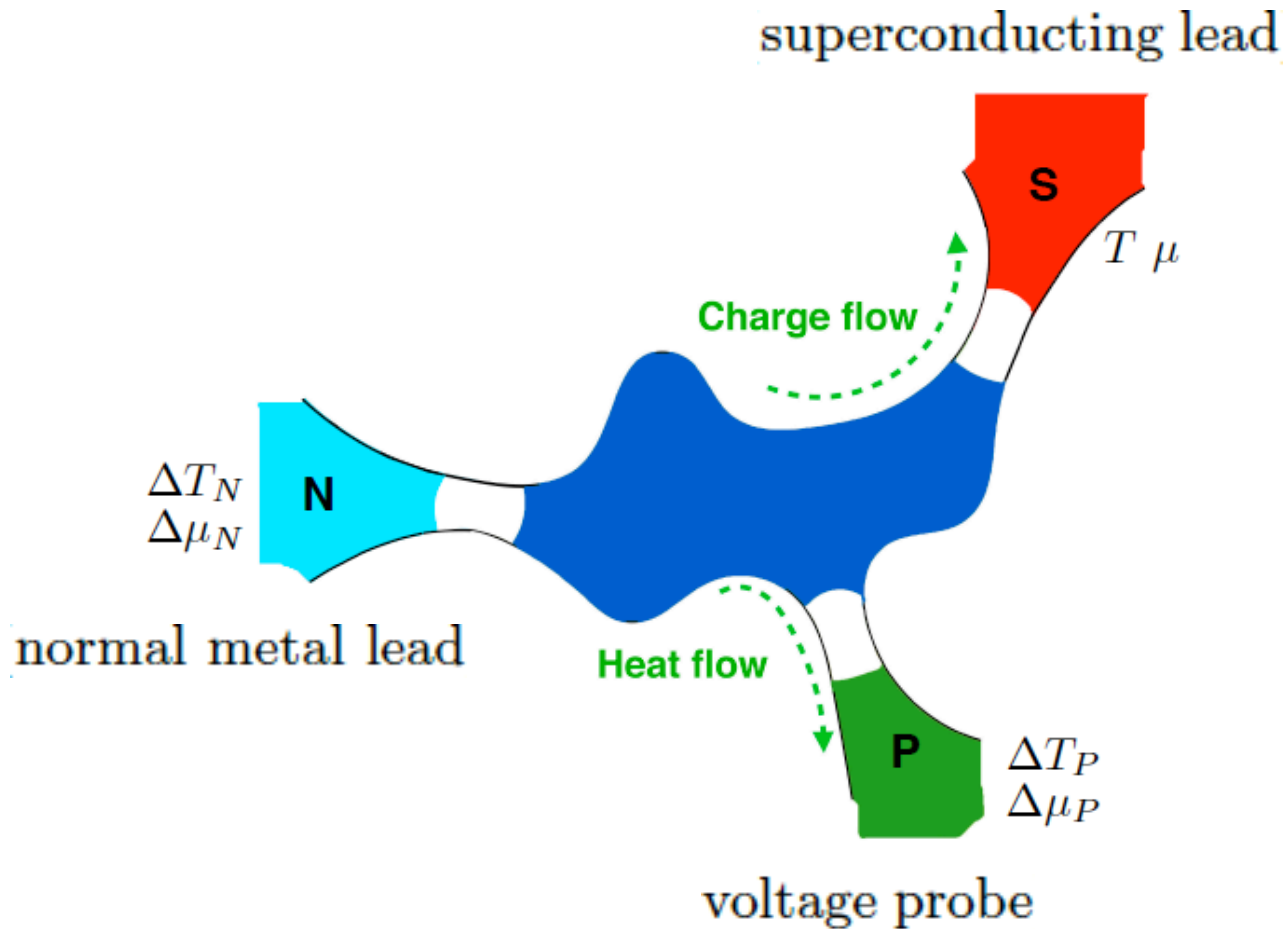
Possibility to exploit additional terminals to **decouple charge and heat flows** and improve thermoelectric efficiency



The third terminal is **not necessarily a probe**

(F. Mazza, R. Bosisio, G. B., V. Giovannetti, R. Fazio, F. Taddei, New J. Phys. **16**, 085001 (2014))

Heat-charge separation



Improved thermoelectric performances (in the low-temperature Sommerfeld regime)

(F. Mazza, S. Valentini, R. Bosisio, G.B., R. Fazio, V. Giovannetti, F. Taddei, PRB **91**, 245435 (2015))

Open problems

To combine thermal rectification with thermoelectric power generation or cooling

Investigate strongly-interacting systems close to **electronic phase transitions**

In **nonlinear regimes** restrictions due to Onsager reciprocity relations might be overcome

Investigate **time-dependent driving**